Active faulting and deep-seated gravitational slope deformation in carbonate rocks (central Apennines, Italy): a new "*close-up*" view

Luca Del Rio[a], Marco Moro[b], Michele Fondriest[c], Michele Saroli[d], Stefano Gori[b], Emanuela Falcucci[b], Andrea Cavallo[e], Fawzi Doumaz[b], Giulio Di Toro[a,b]

[a] Dipartimento di Geoscienze, Università degli Studi di Padova, Via G. Gradenigo 6, 35131 Padua, Italy

[b] Istituto Nazionale di Geofisica e Vulcanologia (INGV), Via di Vigna Murata 605, 00143 Rome, Italy

[c] Institut des Sciences de la Terre (ISTerre), Universitè Grenoble Alpes, 1381 Rue de la Piscine, 38610 Gières, Francia [d d] Università degli Studi di Cassino, via Sant'Angelo in Theodice, 03043 Cassino, Italy

[e] Laboratorio tecnologico multidisciplinare CERTEMA, Grosseto, Italy.

Keypoints:

- Slip surfaces cutting carbonate rocks in the Central Italian Apennines accommodate both normal faulting and DGSDs
- DGSDs are the result of gravity-induced re-activation of faults and fractures located at the footwall of normal seismogenic faults
- Deformation mechanisms associated to normal faulting and DGSDs are cataclasis and pressure-solution active at low ambient temperatures

Keywords: active faults, deep-seated gravitational slope deformation, earthquakes, slip surfaces, cataclasites, carbonates

Correspondence to: L. Del Rio, *Luca.delrio@studenti.unipd.it*

ORCID: *https://orcid.org/0000-0002-6648-9641*

Abstract

Active faulting and Deep-seated Gravitational Slope Deformation (DGSD) constitute common geological hazards in mountain belts worldwide. In the Italian central Apennines, km-thick carbonate sedimentary sequences are cut by major active normal faults which shape the landscape generating intermontane basins. Geomorphological observations suggest that the DGSDs are commonly located in the fault footwalls.

We selected five mountain slopes affected by DGSD and exposing the footwall of active seismic normal faults exhumed from 2 to 0.5 km depth. We combined field structural

analysis of the slopes with microstructural investigation of the slipping zones from the slip surfaces of both DGSDs and major faults. The collected data show that DGSDs exploit pre-existing surfaces formed both at depth and near the ground surface by tectonic faulting and, locally, by gravitational collapse. At the microscale, the widespread compaction of micro-grains (e.g., clasts indentation) forming the cataclastic matrix of both normal faults and DGSDs is consistent with clast fragmentation, fluid-infiltration and congruent pressure-solution mechanisms active at low ambient temperatures and lithostatic pressures. These processes are more developed in the slipping zones of normal faults because of the larger displacement accommodated.

We conclude that in carbonate rocks of the central Apennines, DGSDs commonly exploit pre-existing tectonic faults/fractures and, in addition, localize slip along newly formed fractures that accommodate deformation mechanisms similar to those associated to tectonic faulting. Furthermore, the exposure of sharp slip surfaces along mountain slopes in the central Apennines can result from both surface seismic rupturing and DGSD or by a combination of them.

1. Introduction

Deep-seated Gravitational Slope Deformations (DGSDs) are large and slow rock-mass movements (slip rate of few mm/yr) commonly affecting the entire relief slope and involving ~ 200-300 m thick rock volumes, with relatively small displacements compared to the slope dimensions (Agliardi et al., 2001, 2012; Dramis & Sorriso-Valvo, 1994; Varnes, 1978; Zischinsky, 1966, 1969). Unlike other types of landslides, DGSDs commonly lack of clearly defined boundaries (Crosta et al., 2013). The most common DGSDs are produced: 1) by rock-mass movements that split in the upper slope portion and bulges from depths in the lower one by slipping along hundreds of meters high and steep slopes (i.e., Sackung DGSD; Agliardi et al., 2012; Hermann et al., 2000; Zischinsky, 1969) and 2) by lateral spreading in areas where a thick-bedded and gently dipping sedimentary succession overlies a less competent unit (Agliardi et al., 2012; Jahn, 1964; Zischinsky, 1969). Peculiar morphologies associated to DGSDs are double crest ridges, ridge top grabens, scarps and counterslope scarps, ridge-parallel trenches, tension cracks and bulging slopes (Agliardi et al., 2001, 2012). Several natural factors, and their interaction, control the formation and trigger these large slope instabilities, such as the lithostratigraphic and structural setting (Agliardi et al., 2001; Ambrosi & Crosta, 2006; Hermann et al., 2000; Mariani and Zerboni, 2020), the topographic relief and the state of the stress (Ambrosi &

Crosta, 2006, 2011; Martel, 2006; Molnar, 2004), weather and climate (Agliardi et al., 2001; Evans & Clague, 1994;) and seismic faulting (McCalpin, 1999; Moro et al., 2007; Jibson et al., 2004). Significant natural hazards are associated to DGSDs (Ambrosi and Crosta, 2006; Dramis & Sorriso-Valvo, 1994), in particular because of the sudden acceleration of the slope movements, commonly induced by seismic faulting (Chigira et al., 2010; Moro et al., 2007). A large number of DGSDs were documented worldwide since 1990s, in particular in North America, Europe, Japan and New Zeeland (see Fig. 1 from Panek & Klimes, 2016). Italy is one of the countries in which DGSDs were largely monitored and reported, both in Alps (Agliardi et al., 2001, 2012, 2020; Ambrosi & Crosta, 2006; Crosta et al., 2013; Mariotto & Tibaldi, 2015) and Apennines (Arignoli et al., 2010; Bianchi Fasani et al., 2014; Della Seta et al., 2017; Esposito et al., 2007; Galadini, 2006; Mariani and Zerboni, 2020; Moro et al., 2007, 2009, 2012; Gori et al., 2014).

In the central Apennines, the main controlling factor of the formation and triggering of DGSDs is the energy relief produced by the large number of active, often seismogenic, normal faults (Galadini, 2006; Moro et al., 2007; Fig. 1), with contribution of the regional uplift (more than 1000 m during Quaternary, D'Agostino et al., 2001) and of the interglacial-glacial climate changes (Giraudi, 2001). Active normal faulting affects the Apennines since Late Pliocene (e.g., Barchi et al., 2000; Boncio et al., 2004; Calamita et al., 1994; Elter et al., 1975; Galli et al., 2002; Galadini & Galli, 1999, 2000; Galadini et al., 2000; Moro et al., 2013 Pantosti et al., 1996; Valensise & Pantosti, 2001). The Quaternary activity of normal faults is documented by the displacement of fluvio-lacustrine deposits filling intermontane basins (Galadini, 1999) and by the number of historical earthquakes which hit the area (e.g., 1703 M_w 6.8 L'Aquila earthquake; 1915 M_w 7.1 Avezzano earthquake; 2009 M_w 6.1 L'Aquila earthquake; EWG, 2010; Rovida et al., 2020). In the last 25 years, paleo-seismological and geophysical analyses focused on the mapping and on the assessment of the seismic hazard associated to these active faults. These interdisciplinary studies yielded also information about the length, Quaternary throw, slip rate and earthquake recurrence intervals of the faults (e.g., Barchi et al., 2000; Calamita et al., 2000; Falcucci et al., 2016; Galadini et al., 2003; Galadini & Galli, 2000; Morewood & Roberts, 2000; Pizzi et al., 2002; Roberts & Michetti, 2004). Field structural investigations of the major (up to 15-20 km long) exhumed seismogenic fault surfaces cutting carbonate rocks documented in several cases the presence of a belt of up to hundreds meter-thick damage zones bounding meter-thick fault cores accommodating most of the total displacement (Caine et al., 1999) and containing multiple cm- to mm-thick principal

slipping zones cut by sharp (where karstified) or polished to “mirror-like” (where fresh) slip surfaces (Agosta and Aydin, 2006; Demurtas et al., 2016; Ferraro et al., 2019; Fondriest et al., 2013, 2015, 2020; Siman-Tov et al., 2013).

Recent paleo-seismological, geological and geomorphological observations pointed out that some outcropping sharp scarps cutting the central Apennines carbonate rocks, commonly interpreted as surface expression of seismic faulting, possibly accommodate also DGSDs (Moro et al., 2009, 2012; Gori et al., 2014). In the central Apennines, the slip surfaces associated to DGSDs or faults, respectively, should be exhumed from different depths (0 to few-hundred meters for DGSDs, 0 to 3 km for active faults), and formed and active over a different range of (1) temperatures (< 15 °C for DGSDs, 0-60 °C for faults assuming a geothermal gradient of ca. 20°C/km, typical for the central Apennines; Mancinelli et al., 2019), (2) lithostatic pressure (< 15 MPa for DGSDs, 0-80 MPa for faults) and (3) slip rates (usually < mm/s for DGSDs, up to ~ 1 m/s for seismic faults). Such large differences in loading conditions should result in the formation of distinctive secondary fault/fracture networks, possibly recognizable at the outcrop scale, and microstructures of the slipping zones.

Here we discuss four cases of DGSDs located at the footwall of active seismogenic normal faults and one case of a normal fault bordering a relatively small intermontane basin (Italian central Apennines, Figs. 1, 2). We analyzed the fracture network at the footwall of the major slip surfaces and compared the microstructures of the slipping zones of the DGSDs with the ones of the associated seismic normal faults to interpret the deformation mechanisms active during slip and the formation of DGSDs.

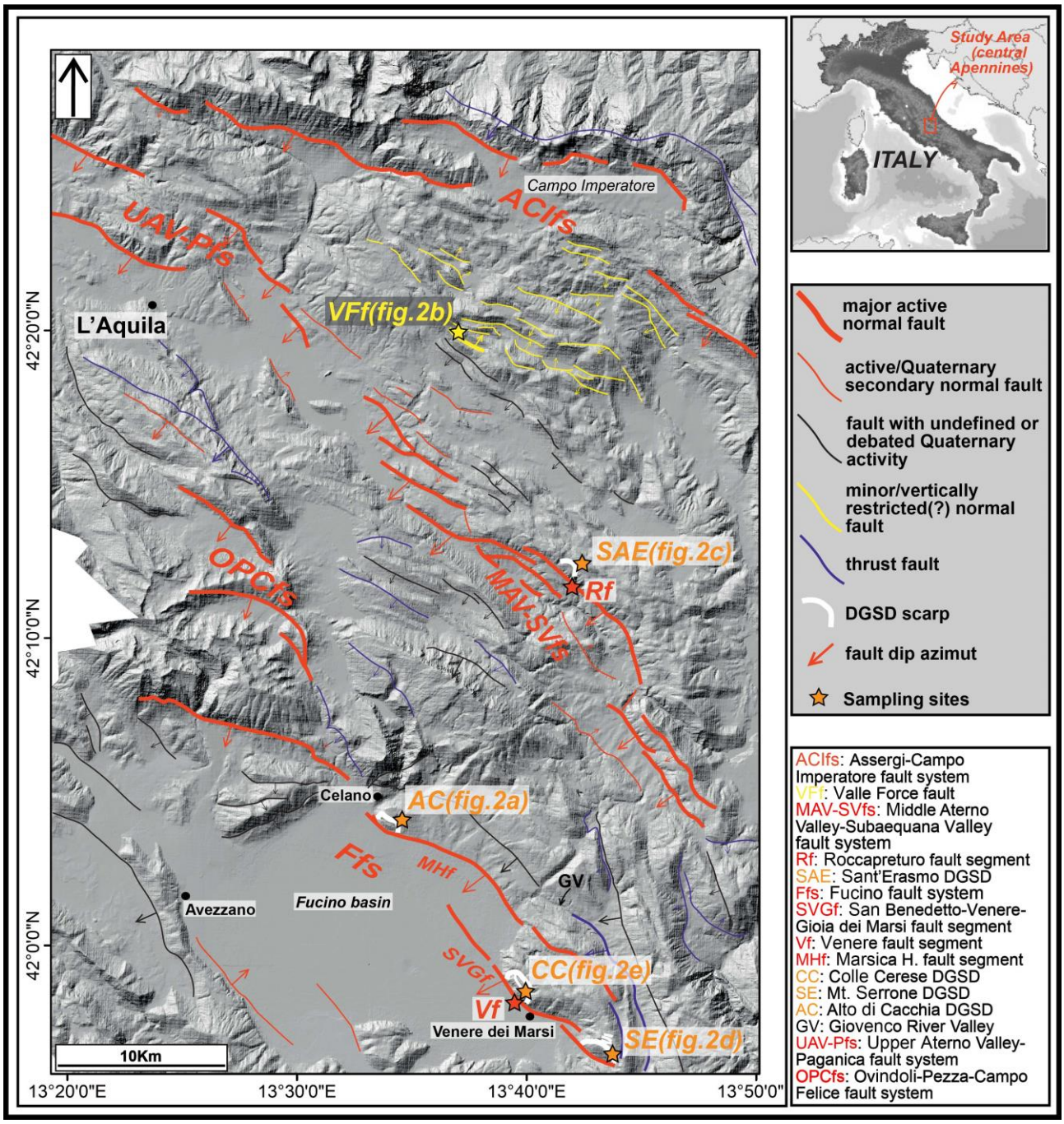

Figure 1: Structural scheme of the study area. Major active normal faults (thick red lines): Assergi-Campo Imperatore fault system (Galli et al., 2002); Middle Aterno Valley-Subequana Valley fault system (Falcucci et al., 2015); Fucino fault system (Galadini and Galli, 1999); Upper Aterno Valley-Paganica fault system (Moro et al., 2013); Ovindoli-Pezza-Campo Felice fault system (Pantosti et al., 1996). Minor/vertically restricted normal faults (black in color) are from D'Agostino et al. (1998) and Falcucci et al. (2015). Deep-seated Gravitational Slope Deformations (DGSDs) are widespread in this region, as well as in all the Apennines (see main text for the references). Here are shown the DGSDs discussed in this work. The Alto di Cacchia, Sant'Erasmo, Colle Cerese and Mt. Serrone DGSDs (White in color) are all located at the footwall of major active normal faults; the Valle Force fault (yellow in color) is ca. 2 km long along-strike. Stars indicate the sampling sites of the studied slipping zones (next figures).

2. Geological setting

The structural setting of the central Apennines is the result of the superimposition of three main tectonic phases. From the Late Triassic to the Middle Jurassic, an extensional phase affecting the whole Central-Mediterranean area associated to the opening of the Liguria-Piedmont Ocean (Western Tethys) lead to the fragmentation of the Adriatic plate paleo-margin. The diffuse normal faulting brought to the drowning of some sectors of the carbonate platforms and the formation of basins (e.g., Carminati & Doglioni, 2012; Castellarin et al., 1978; Cosentino et al., 2010). In the platform areas, the deposition of shallow-water limestones continued till the Late Cretaceous and re-started in the Middle Miocene (i.e., “Paleogene Hiatus”, Cosentino et al. 2010; Damiani et al., 1992; Parotto & Praturlon, 1975). In the Late Miocene, the platform areas were involved in the Apennine orogenesis, caused by the NE verging convergence between the Adriatic and European plates (Bally et al., 1988; Carminati et al., 2012; Cosentino et al., 2010; Patacca et al., 1992a). The study area represents a platform carbonate sector of the Adriatic plate paleo-margin which was involved in the Apennine orogenesis. The slab-rollback of the subducting Adriatic plate caused the back-arc opening of the Tyrrhenian Sea and the migration toward E-NE of the Apennine fold and thrust belt (Carminati et al., 2012; Cipollari et al.,1999a; Doglioni, 1995; Malinverno & Ryan, 1986; Vezzani & Ghisetti, 1998). From the Pliocene till present, extensional tectonics accommodated the migration of the chain towards the E-NE. In the central Apennines, the current extensional phase started in the Middle Pleistocene. The extension is accommodated by normal faults which cut and locally exploit the inherited Miocene-Early Pleistocene thrusts and the earlier Mesozoic normal faults (Elter et al., 1975; Vezzani et al., 2010). The extensional Plio-Quaternary activity was responsible for the formation of numerous intermontane basins, filled by lacustrine and alluvial deposits and bordered by large normal faults (Bosi et al., 2003; Cavinato et al., 2002; Fig. 1).

The outcropping main active faults strike NW-SE and dip towards SW, consistent with the NE-SW direction of extension (> 3 mm/yr of extension rate) documented by geodetic data (Serpelloni et al., 2005; D’Agostino et al., 2011), focal mechanisms (Chiaraluce et al., 2003) and borehole breakout data (Mariucci & Muller, 1999). These normal faults cut the pre-Miocene carbonate sequences (> 4 km of stratigraphic thickness in some areas, excluding thickening due to thrust activity, Tozer et al., 2002), and cause destructive historical earthquakes up to M_w 7.1 (e.g., Avezzano 1915; Fig. 1).

2.1 Stratigraphic and geomorphological characterization of the study cases

Remote sensing, photogeological and geomorphological interpretations allowed us the identification of double crest lines, scarps and counterslope scarps, slope-parallel trenches and open fractures associated to DGSDs in the central Apennines, located in the footwall of large seismogenic faults (Moro et al., 2009, 2012). The four selected DGSDs are described below based on their stratigraphic, geomorphic and geological setting, starting from the Alto di Cacchia DGSD. For comparison, the case of the Valle Force normal fault is described after the Alto di Cacchia DGSD.

Alto di Cacchia DGSD. Alto di Cacchia is a flat top hill (950 m a.s.l.) located few km to the east of the Celano town. The hill is about 500 m long along the NW-SE direction and is laterally confined to WNW by the Fucino Basin and to ESE by a fluvial incision. The Alto di Cacchia hill is bordered to SW by the NW-SE oriented “Marsicana Highway” fault segment (Mf) (Galadini and Galli, 1999), belonging to the Fucino seismogenic fault, which puts in contact early Quaternary Cupoli/Aielli continental units (Bosi et al., 2003) and the underlying Cretaceous platform carbonates in the footwall with the Quaternary lacustrine deposits of the Fucino Basin in the hangingwall (Fig. 2a). The DGSD affects the uppermost portion of the Cupoli unit (~ 120 m of maximum thickness), which consists of Early Pleistocene gravels intercalated with sands and silt deposited in lacustrine and fluvial environments (Fig. 2a). The Cupoli unit is embedded into the Aielli Conglomerates (~ 400 m thick) formed by blocks of carbonate rocks within a silty and clayey matrix (Bosi et al., 2003; Bosi & Messina, 1991). The geomorphological structure of Alto di Cacchia was interpreted by us as a DGSD based on the following evidences: (1) the continental deposits of the Alto di Cacchia are cut by a curved and discontinuous but sharp scarp which borders a ~ 200 m wide and ~ 500 m long depression interrupting the regular sub-horizontal top of the hill; (2) the presence of scarps and trenches cross cutting the sub-horizontal continental strata and a characteristic double crest line topographic morphology typical of DGSDs (Fig. 2a); (3) the described landforms affect only a sector of Alto di Cacchia, as no other lineaments or scarps affect the hill toward SE.

Valle Force fault (normal fault bordering a small and narrow basin). The Valle Force fault (< 2 km in length along-strike), selected for comparison with typical DGSDs cases, is one of the several NE dipping normal faults bordering small and narrow

intermontane basins located in the area between the Campo Imperatore basin, to NE, and the Middle Aterno Valley, to SW (D'Agostino et al., 1998; Falcucci et al., 2015; Galadini & Messina, 2004; Fig. 1). This "Basin and Range" like area consist on NE dipping (25º-40º of dip angle) rotating antithetic normal faults bounding southward the tilted blocks, which likely detach onto a splay of the Gran Sasso thrust system at relatively shallow depth (~ 2 km). The presence of a shallow-seated detachment fault is supported by the very limited dimensions of the tilted blocks (D'Agostino et al., 1998; Falcucci et al., 2015). The Valle Force fault is located just north-east of the Barisciano village (Fig. 2b). The fault juxtaposes the Mesozoic carbonate platform ("Calcari a Coralli e Diceratidi" fm.) forming the footwall ridge (~ 1200 m a.s.l.) with Pleistocene-Holocene colluvial deposits and Lower Pleistocene slope-derived calcareous breccias with pink matrix ("Brecce Mortadella" in Demangeot, 1965 or "Brecce di Fonte Vedice" in Bosi & Messina, 1991) whose deposition was coeval to the normal activity of the fault (D'Agostino et al., 1998).

Sant'Erasmo DGSD. The Sant'Erasmo DGSD is located just northwest of the Roccapreturo village, in the Middle Aterno River Valley. The sliding of the rock-mass along the NW-SE oriented major scarp (< 1 km long) produced an about 500 m wide depression on top of the unstable slope associated to a series of uphill facing scarps (Fig. 2). The lower one (< 400 m long) affects the western flank of the Mt. Acquaro, located in the footwall of the Roccapreturo normal fault segment (Rf; Fig. 2), which is the longest segment of the ~ 30 km-long Middle Aterno Valley-Subequana Valley fault system (Falcucci et al., 2011, 2015; Fig 1). The fault is about 10 km long along-strike and the estimated Quaternary displacement is about 270 m, while the minimum slip rate and earthquake recurrence interval range from 0.23 to 0.34 mm/yr and 5340 to 1758 yrs, respectively (Falcucci et al., 2015). A small depression (< 100 m wide) filled by Pleistocene-Holocene sub-horizontal breccias with pink-orange matrix, overlying Early Cretaceous platform carbonates ("Calcari a Rudiste e Orbitoline" fm.) dipping at ~ 25º to NE, is associated to this counterslope scarp (Fig. 2c). The large depression associated to the major scarp and the counterslope scarp partially balancing and arresting the sliding of the rock-mass involved were interpreted by us as morphological features indicative of the occurrence of a DGSD.

Serrone DGSD. The Mt. Serrone DGSD, located just northeast to the Gioia dei Marsi village, is a gravitational rock-mass deformation accommodated by several shear surfaces

affecting the western slope of Mt. Serrone (~ 1350 m a.s.l.). The NE dipping major scarp accommodating the DGSD is antithetic with respect the San Benedetto-Gioia dei Marsi normal fault segment, belonging to the larger Fucino seismogenic fault, which borders the south-eastern sector of the Fucino Basin (Fig. 1, 2d). The depression associated to the DGSD (< 400 m wide) is filled with colluvial and talus deposits deriving from the erosion of the Cretaceous carbonates (~ 20º of average dip to NE) forming the Mt. Serrone. The Cretaceous carbonates are juxtaposed to the Val Roveto flysch by the thrust bordering the eastern side of the Giovenco Valley (Fig. 1; Ghisetti & Vezzani, 1998). Here, several morphological features indicative of a DGSD, such as scarps and counterslope scarps, slope-parallel trenches, open fractures and linear alignments of NW-SE oriented small depressions were identified through photogeological and field analyses (Moro et al., 2009, 2012).

Colle Cerese DGSD. The Colle Cerese hill (~ 1100 m a.s.l.) is located just northeast to the Venere village. An impressive double crest ridge interrupts the regular morphological slope continuity of the hill towards the Fucino Basin (Fig. 2e). The gravitational activity is triggered by the San Benedetto-Gioia dei Marsi fault segment (SGf, in this area called Venere sector) and cropping out at the base of the slope. The activity of this fault increases the local relief generating the gravitational instability (Moro et al., 2009; Stramondo et al., 2005). The SGf (about 10 km long along-strike) re-activated together with the “Marsicana Highway” fault segment and other faults belonging to the Fucino fault system (1.5-2.4 mm/yr of total minimum slip rate; Carafa et al., 2020) during the 1915 M_w = 7.1 Avezzano earthquake (Rovida et al., 2020; Ward and Valensise, 1989). The SGf has an estimated maximum throw ranging from 800 m to 1300 m (Cavinato et al., 2002; Roberts & Michetti, 2004) and a minimum slip rate of 0.24-0.29 mm/yr (Galadini & Galli, 1999). The Colle Cerese hill is carved into NE dipping Cretaceous platform carbonates, which are juxtaposed by the SGf to the Quaternary lacustrine deposits filling the Fucino Basin (Ghisetti & Vezzani, 1998). The large depression between the two crests (> 1 km long and ~ 400 m wide) is filled with Pleistocene-Holocene fluvio-lacustrine and talus deposits (Moro et al., 2009; Fig 2e). The double crest ridge morphology is a clear evidence of a deep gravitational slope instability affecting the Colle Cerese hill. Other evidences of gravitational deformation, such as counterslope scarps, slope-parallel trenches and open fractures, were described in Moro et al. (2012).

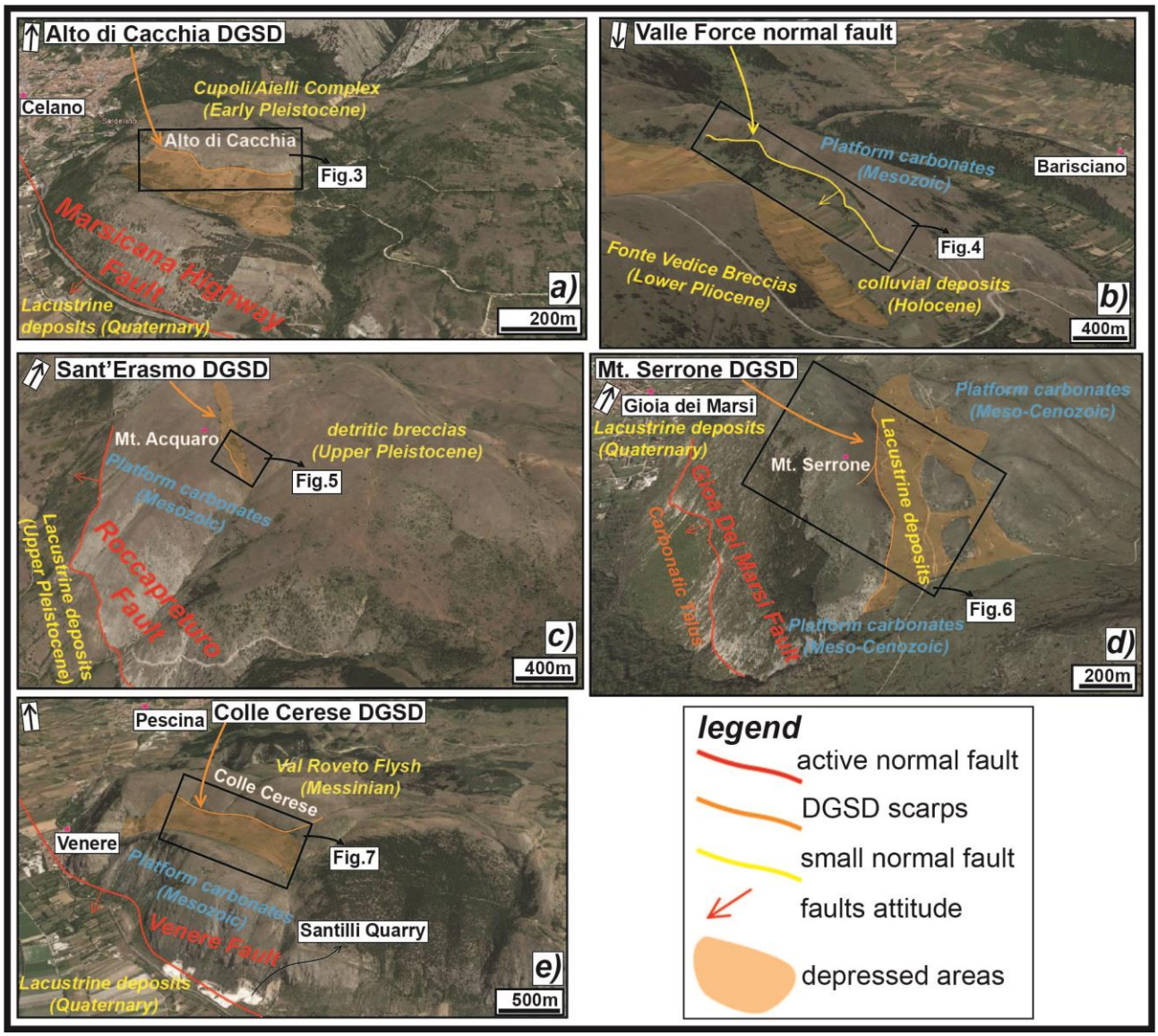

Figure 2: Panoramic view of the five case studies: a) Alto di Cacchia DGSD, located at the footwall of the "Marsicana Highway" normal fault segment; b) Valle Force normal fault, bordering a small and laterally confined basin; c) Sant'Erasmo DGSD at the footwall of the Roccapreturo normal fault segment; d) Mt. Serrone DGSD, at the footwall of the San Benedetto-Gioia dei Marsi normal fault segment; e) Colle Cerese DGSD at the footwall of the San Benedetto-Gioia dei Marsi normal fault segment (Venere sector). The lateral continuity of the DGSDs is limited compared to the associated faults. Images from Google Earth.

3. Methods

Photogeological and geomorphological analyses of the study area allowed us to identify peculiar structural features associated to DGSDs. The latter were investigated in the field through detailed structural geology surveys of the host rocks and of the fault and fracture network at the footwall of the major slip surfaces. We distinguished joints from open cracks and measured the attitude and kinematics (i.e., rake) of the major slip surfaces where possible. The structural data were reported in topographic maps at 1:1000

scale, produced by exploiting the aerial photos (spatial resolution of 10x10 meters) provided by the Abruzzi Geoportal (http://geoportale.regione.abruzzo.it/Cartanet) and plotted as poles into a stereonet (Schmidt equal area, lower hemisphere). In the case of Alto di Cacchia, Sant'Erasmo and Colle Cerese DGSDs and of the Valle Force fault we also used high-resolution orthomosaics produced by stitching hundreds of images (we used Agisoft Metashape Pro and Pix4D software) taken at 100-150 meters from the ground with a drone (Phantom 4 Advanced and MAVIC 2 Pro). Regarding the collected samples, Syton-polished thin sections of the slipping zones associated to the major and secondary slip surfaces were produced by cutting the samples perpendicular to the slip surface and parallel to the slip direction (where recognizable, otherwise along the dip direction). The thin sections where photo-scanned at high resolution (4000 dots per inch) scanning both in plane and cross polarized nicols and observed under the Optical Microscope (OM) and Scanning Electron Microscope (SEM). The scans of all the thin sections were edited using specific tools of Adobe Photoshop (Ps) to highlight the clast shapes, the presence of minor fractures and veins and the texture of the fine matrix surrounding the clasts.

Most thin sections were investigated for microstructural analysis with the Scanning Electron Microscope CamScan MX3000 (resolution 300 nm in back-scatter electrons) installed at the Dipartimento di Geoscienze (Padua Univ.) and with the Field Emission SEM (FESEM) Merlin Zeiss (resolution 200 nm in back-scatter electrons) installed at CERTEMA laboratory (Grosseto, Italy). The Images were taken in backscattered electron mode (BSE) with an acceleration voltage of 8-10 kV and a working distance of 4.7-6.1 mm.

4. Results

4.1 Structural architecture

Here below we present data regarding the fault/fracture network at footwall of the five selected case studies. We distinguished among (1) slip surfaces or faults as they include the slipping zone and damage zone beneath, (2) open fractures (or cracks) and (3) closed fractures (or joints) (Pollard and Aydin, 1988). Open and closed fractures do not accommodate measurable slip in the field but are crucial to assess the extension and structure of the footwall damage zones.

Alto di Cacchia (DGSD affecting Pleistocene deposits). The Alto di Cacchia DGSD is limited by a ~ 500 m long and discontinuous major sharp scarp dipping on average at ~

70º and crosscutting sub-horizontal (4º to 15º of dip) conglomerates mainly dipping toward NNW-NNE (Figs. 2a, 3a-e). The scarp is karstified and locally smoothen by the rainwater flow. In the north-western tip, the scarp has a lateral continuity of ~ 100 m and is up to 3 m high (fig. 3b, d). Here, the scarp surface appears sharp with some more polished patches, including slickenlines plunging 80º East (almost pure normal dip-slip, Fig. 3d). Two smaller scarps < 1 m high and ~ 50 m long are discontinuously outcropping within the upper depression of the DGSD (fig. 3c, f). Patches of less cemented likely-Holocene deposits filling the upper depression lean on and partially preserve these scarps by processes of surficial alteration (Fig. 3f).

A large number of open fractures (from 1 to 12 cm of aperture) dipping > 70° affect the sub-horizontal cemented conglomerates outcropping at the footwall of the major scarp, while few and short closed fractures were measured. The strike of both open and closed fractures is very scattered (Fig. 3a), and the surfaces of the largest fractures often follow the morphology of the largest pebbles of the conglomerate (Fig. 3e). The smallest open fractures are filled by recent unconsolidated deposits.

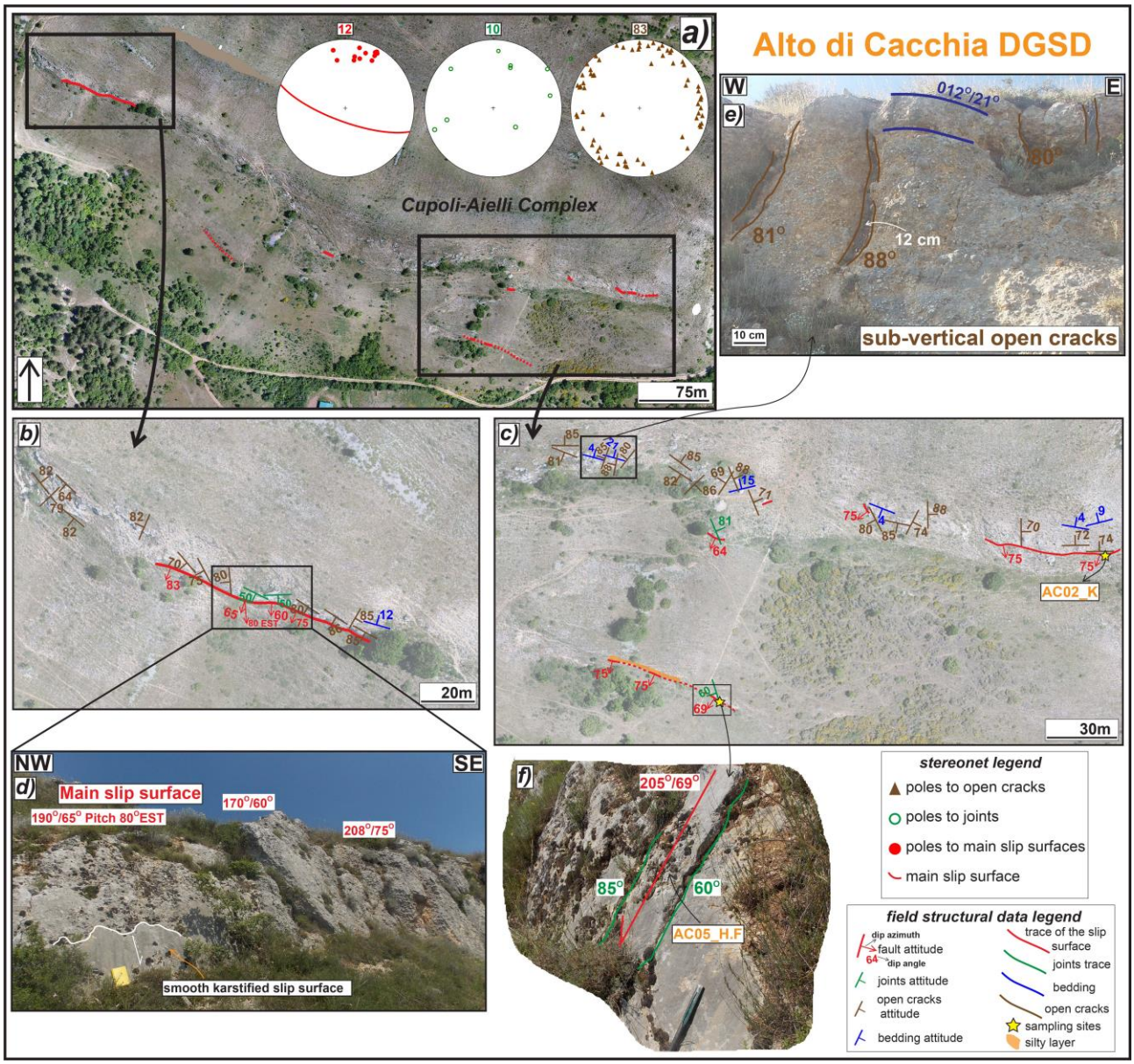

Figure 3: structural sketch map of the Alto di Cacchia DGSD. a) Orthomosaic of the major and secondary scarps crosscutting the flat top hill carved into the Pleistocene conglomerates of the Cupoli Unit. b) Zoom on the north-western tip, where the major karstified scarp outcrops for ~100 m of length along-strike, locally appearing smooth (d). c) Zoom on the south-eastern sector, where a secondary hangingwall sharp scarp outcrops for ~ 50 m, including patches of likely-Holocene sediments leant on the surface (f) (Sample AC05_H.F). e) Sub-vertical open cracks crosscutting sub-horizontal conglomeratic strata and partially following the morphology of the largest pebbles.

Valle Force (minor and vertically confined normal fault). The Valle Force normal fault has a very sharp scarp outcropping continuously for about 1.5 km along-strike with an average dip of ~ 50º and reaching ~ 8 m of height in the middle sector (Fig. 4a-c, e). The fault juxtaposes Cretaceous platform carbonates in the footwall with colluvial deposits filling the basin (Pleistocene-Holocene) and Lower Pleistocene calcareous breccias in the hangingwall. Close to the north-western tip, secondary scarps dipping 60º-80º, sub-parallel to the major one, displace the hangingwall breccias, possibly associated to gravitational instability (Fig. 4d). Just south-east along-strike, the fault scarp dextrally steps involving the Early Pleistocene breccias into the relay zone (Fig. 4e). In the middle sector of the fault, small patches of the hangingwall breccias cover the major scarp, thus preserving the fault core (Fig. 4f). Where the breccias are removed, the fault surface appears ultra-polished (Fig. 4f). A relatively large number of joints cut the fault surface and the footwall carbonates, which sporadically outcrops along the fault strike (stereonets in Fig. 4a). Both joints and the few open cracks have a relatively large scatter in dip angle (e.g., it ranges from 80º to 45º, as shown in Fig. 4a, g) and are arranged in conjugated sets dipping on average (dip angle/dip azimuth) 50º/N260º-300º and 50º/N130º-180º.

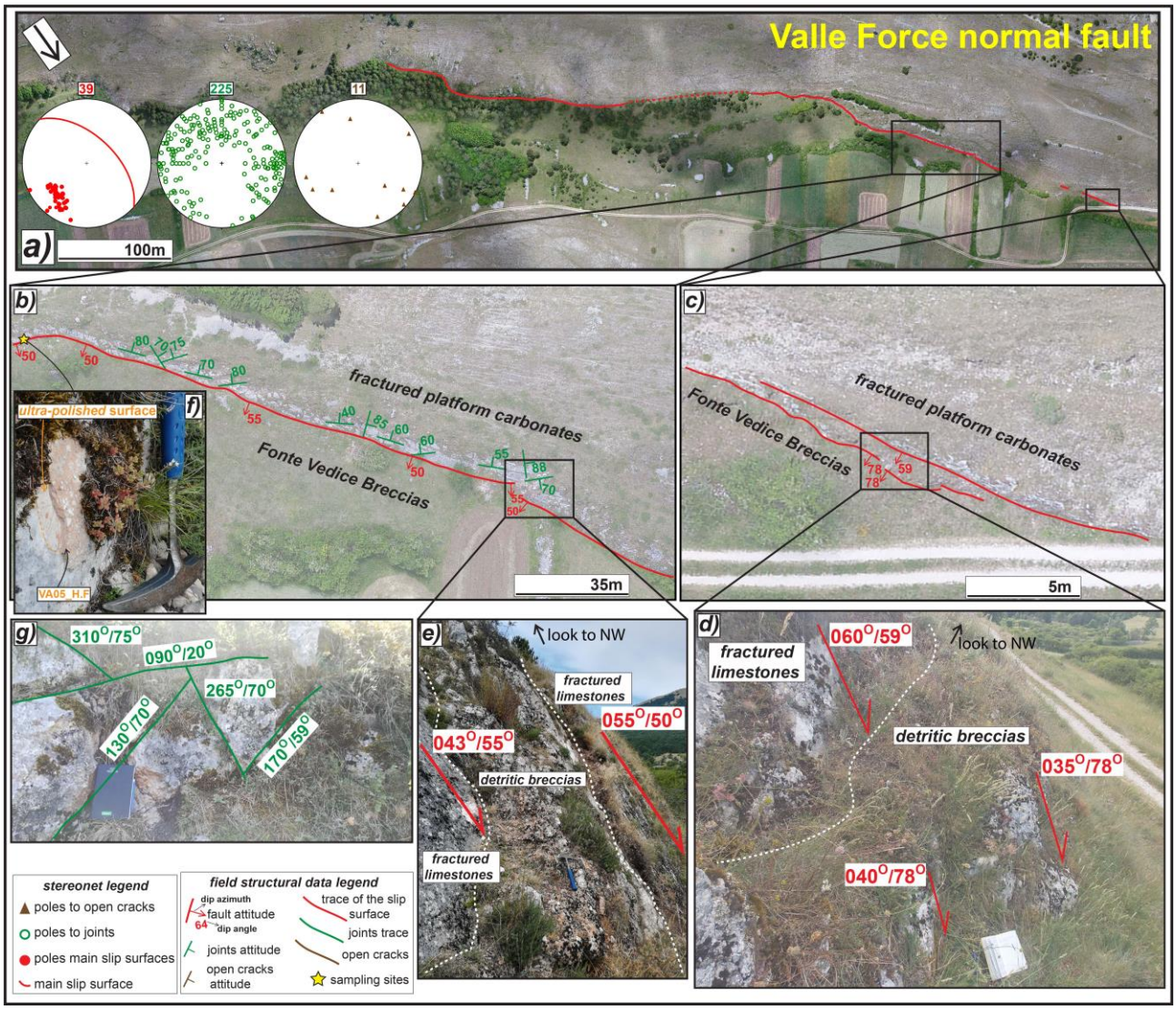

Figure 4: structural sketch map of the Valle Force normal fault. a) Orthomosaic of the main scarp juxtaposing Cretaceous limestones with Lower Pleistocene breccias and Holocene deposits. b) Zoom on the north-western tip, where secondary high angle scarps crosscut the hangingwall breccias (d). c) Zoom on the sharp fault scarp where it dextrally steps involving the hangingwall breccias into the relay zone (e). f) Conjugated joints affecting the fault scarp with different attitude. g) Patch of the hangingwall breccias on the slip surface. The latter appears as ultra-polished where the breccias are removed (sample VA05_H.F).

Sant'Erasmo (DGSD in the footwall of a main seismogenic fault). The Sant'Erasmo DGSD is located at the footwall of the Roccapreturo seismogenic normal fault segment and is limited by an about 700 m long major scarp striking NW-SE, sub-parallel and synthetic to the Roccapreturo fault (Fig. 2c). The field work was conducted on the small counterslope scarp (< 400 m long along-strike and till 3 m high) affecting the eastern slope of the Mt. Acquaro and associated to a small depression filled by Pleistocene breccias with pink-orange matrix and colluvial deposits (Figs. 2c, 5a). The counterslope scarp has an average dip angle of ~ 70º, is strongly karstified and displaces Cretaceous platform

carbonates. At the hangingwall of the scarp, small secondary sub-vertical sharp scarps cut the Pleistocene breccias and form small, possibly gravitational trenches (Fig. 5b). The footwall carbonates are locally intensely fractured and somewhere appear as brecciated (Fig 5c). As in the case of the Valle Force normal fault, a relatively large number of joints affecting the major slip surface and the footwall carbonates were measured compared to the few open fractures (tens of centimeters long and 1-5 cm spaced). Both joints and cracks have a very scattered attitude, with the dip angle ranging from 88º to 15º (Fig. 5a). However, most joints are arranged in two main conjugated sets striking ca. NE (Fig. 5a, d).

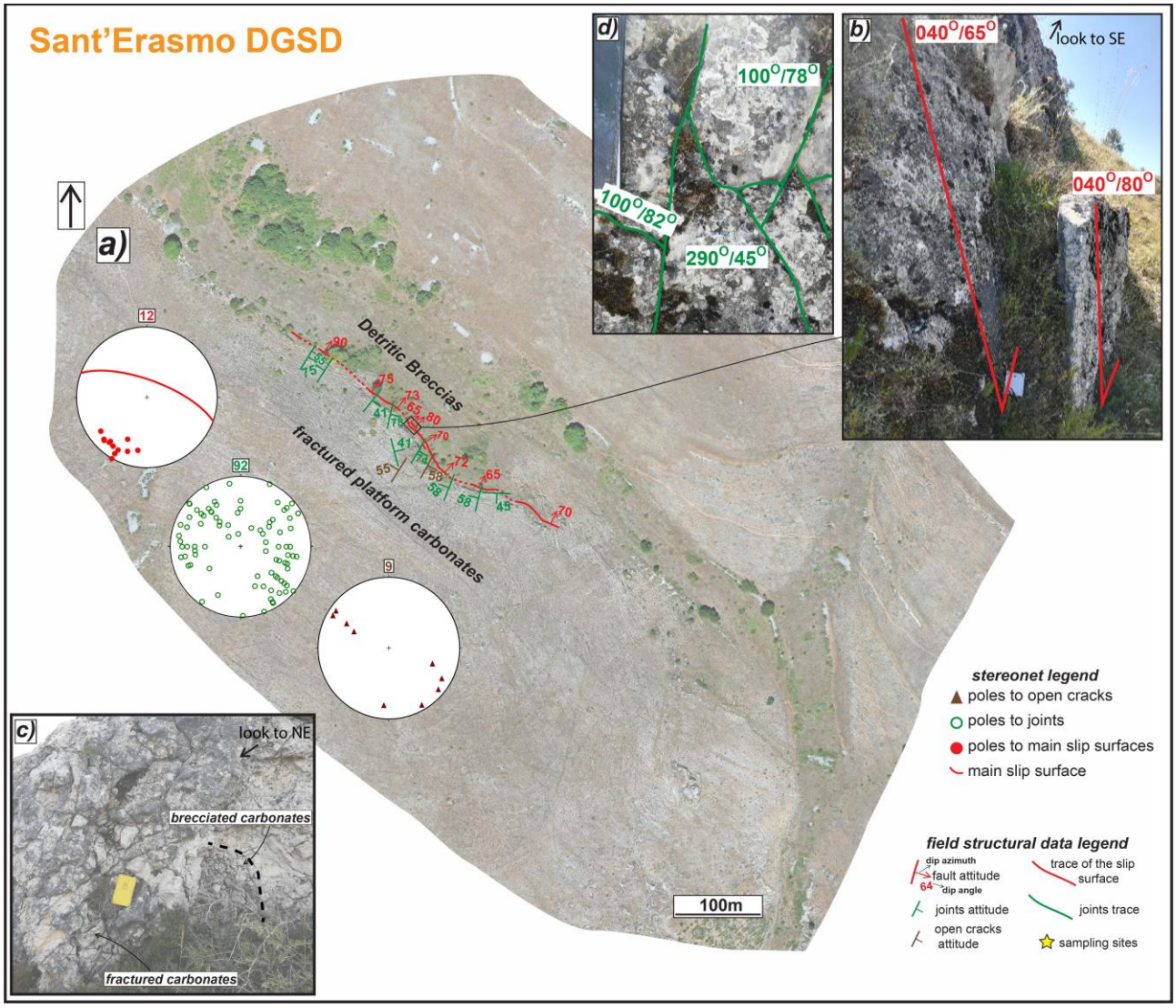

Figure 5: structural sketch map of the Sant'Erasmo DGSD counterslope scarp. a) Orthomosaic of the scarp juxtaposing Cretaceous fractured limestones with Pleistocene-Holocene detritic breccias. b) Major sharp slip surface and a secondary sub-vertical hangingwall scarp crosscutting the breccias and forming a gravitative trench. c) Intensely fractured footwall carbonates, somewhere appearing as brecciated. d) Conjugated joints cut by the major slip surface.

Mt. Serrone (DGSD at the footwall of a main seismogenic fault). This DGSD affects the eastern slope of Mt. Serrone and is limited by a ~ 500 m long sharp scarp displacing sub-horizontal Mesozoic platform carbonates antithetically with respect to the San Benedetto-Gioia dei Marsi normal fault segment (Figs. 2d, 6a-c). In the middle sector, the major scarp sharply outcrops for ~ 200 m along-strike, with a maximum height of ~ 3 m in some sectors and an average dip angle of ~ 50° (Fig. 6a, d). Towards the south-east, the scarp rotates in strike from NW-SE to NNW-SSE and dextrally steps to SE. The right stepped segment appears much more karstified and dips to NE with an average dip of ~ 65° (Fig. 6e), similarly to the north-eastern termination of the scarp. Patches of Holocene poorly cemented deposits filling the upper depression of the DGSD are leant on the slip surface of the left stepped segment (Fig. 6e). In the relay zone between the N-S and NW-SE oriented scarps, several meter-long sub-vertical open fractures (up to 15 cm of aperture) crosscut the carbonate rocks (Fig. 6f). Instead, and similarly to the Sant'Erasmo DGSD case, the closed fractures are scattered in attitude and are arranged into several conjugated sets striking at N280°-330°, with dip angles ranging from sub-vertical to sub-horizontal (Fig. 6a).

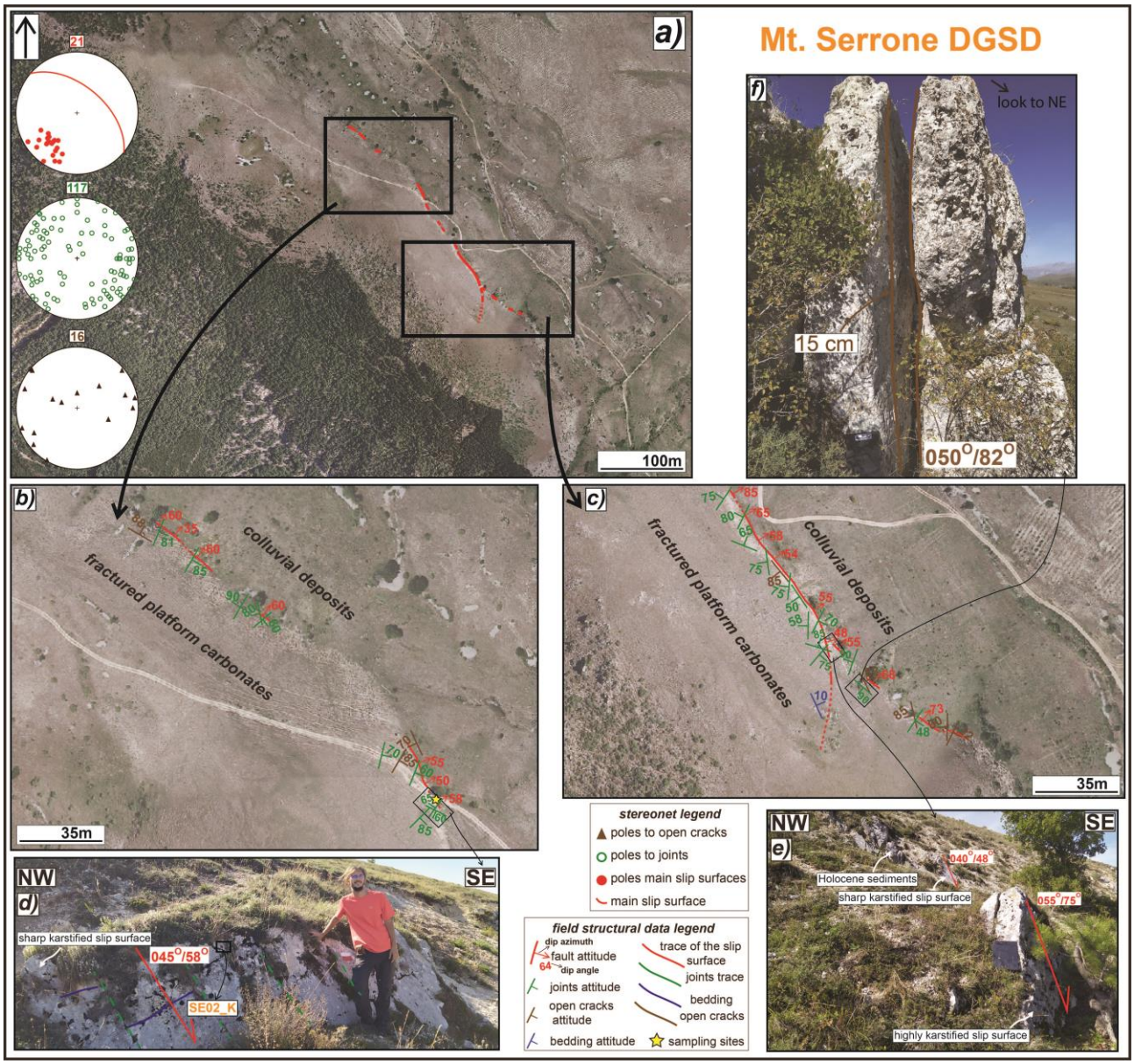

Figure 6: structural sketch map of the Mt. Serrone DGSD. a) Orthomosaic of the major scarp affecting the north-eastern slope of the Mt. Serrone, carved into Mesozoic platform carbonates. b) Zoom on the middle to north-western portion. c) Zoom on the middle to south-eastern portion, where the scarp dextrally steps. d) Detail of the sharp scarp in the middle sector cutting NE dipping carbonates with ~ 45° of dip angle (Sample SE02_K). e) Dextral step between the N-S oriented sharp scarp, locally covered by patches of Holocene cemented sediments, and the much more karstified NW-SE oriented scarp. f) Large sub-vertical open crack affecting the carbonate rocks into the step over zone.

Colle Cerese (DGSD at the footwall of a main seismogenic fault). The Colle Cerese DGSD is located at the footwall of the San Benedetto-Gioia dei Marsi normal fault segment, in the Venere sector, and is limited by an about 1.5 km long major sharp scarp, NW-SE oriented (Figs. 2e, 7a). The field work was conducted in the south-eastern sector of the scarp (Fig. 7b). Here, the slip surface juxtaposes Mesozoic platform carbonates in

436 the footwall with Pleistocene colluvial deposits and unconsolidated breccias filling the large
437 upper depression in the hangingwall. The scarp dips on average ~ 45º and reaches over
438 10 m of height in some sectors (Fig. 7c). Patches of more cemented hangingwall breccias
439 are leant on the slip surface, which is partially preserved by weathering processes (Fig. 7c,
440 d). An about 4-5 cm thick white in color fresh scarp exposure is locally recognized (i.e.,
441 "*nastrino*" or ribbon-like scarp, shown in Fig. 7d). The sub-horizontal carbonates strata
442 appear intensely fractured only close to the major scarp, whereas just few tens of meters
443 back, few and small sub-vertical closed and open fractures affect the latter (Fig. 7e). As in
444 the Sant'Erasmo and Serrone DGSD cases, the joints have scattered attitude and most of
445 them are arranged in conjugated sets striking N290º-340º with dip angles ranging from
446 sub-vertical to sub-horizontal (Fig. 7a, f).

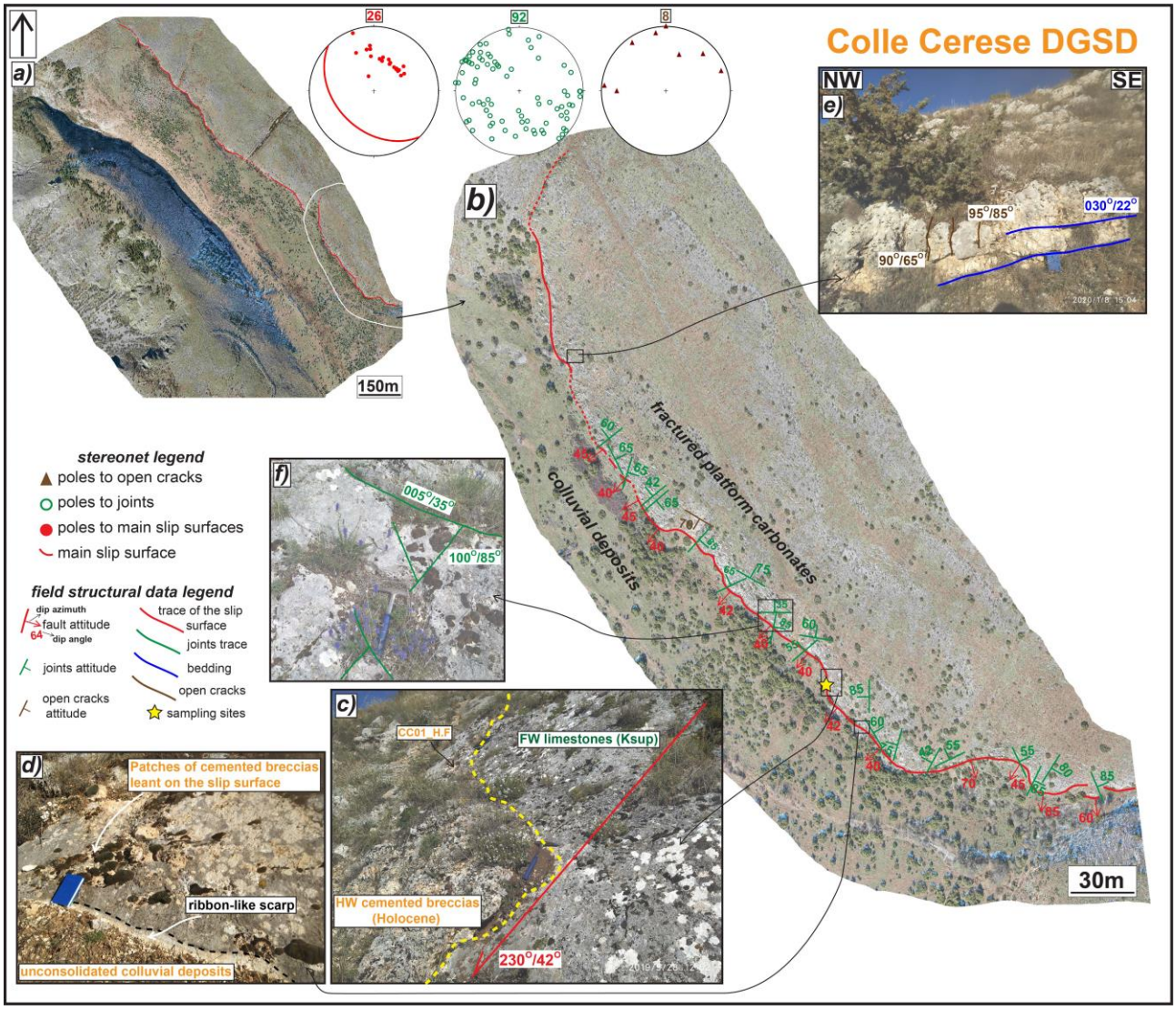

447

448 **Figure 7**: structural sketch map of the Colle Cerese DGSD. a) Orthomosaic of the main scarp affecting the
449 south-western slope of Colle Cerese. b) Zoom on south-eastern sector, where the sharp scarp juxtaposes
450 Cretaceous platform carbonates with Holocene breccias and colluvial deposits with an average dip of ~ 45º

(c) (Sample CC01_H.F). d) Detail of the sharp slip surface locally preserved by patches of cemented breccias and of the ~ 5 cm thick fresh scarp exposure (i.e., ribbon-like scarp). e) Sub-vertical open cracks crosscutting the sub-horizontal carbonate-built strata at footwall. f) Conjugated joints affecting the slip surface, dipping both at high and low angles.

4.2 Microstructures of the slip zones

The microstructures observed in the slipping zones associated to the five selected field cases and, for comparison, of two major fault scarps of the San Benedetto-Gioia dei Marsi and Roccapreturo normal fault segments (Figs. 8-12), are described below following the fault rocks classification of Sibson (1977). Here we indicate the exposed karstified scarps and the scarps preserved by Quaternary hangingwall sediments as the slip surface, whereas the slipping zone (several centimeters thick) consist on variously deformed rocks developed beneath the slip surface, accommodating the bulk of displacement during shearing (Sibson, 2003). Finally, as Principal Slipping Zone (PSZ) we indicate a texturally distinct layer, usually < 1 cm thick (Sibson, 2003), located just beneath the slip surface, on which most of displacement is accommodated.

Alto di Cacchia (DGSD affecting Pleistocene deposits). The slipping zone at the footwall of the major scarp has a cataclastic fabric made of sub-parallel and several mm thick cataclastic and proto-cataclastic layers (sample AC02_K, Fig. 8a). Indeed, the slipping zone is formed by few cm in size sub-rounded clasts (often black in color and difficult to distinguish from the matrix under the optical microscope) and several mm in size angular-to-rounded particles immersed in a dark fine matrix, locally fractured. Close to the slip surface, a ~ 2 mm thick and discontinuous cataclastic layer made of < 1 mm in size angular to sub-rounded grains was identified (Fig. 8a). Under the Scanning Electron Microscope, the fine dark matrix of this layer is composed by sub-micrometric to 5 micrometers in size calcite grains with relatively straight boundaries forming locally triple junctions or separated by sub-micrometric in size pores and grains of apatite or clay minerals with euhedral habit (Fig. 8b). The large size distribution of the calcite grains reminds the one typical of cataclasites (e.g., Sammis, 1987; Storti and Billi, 2004). Some calcite grain boundaries have, instead, irregular and stylolitic aspect, suggesting grain indentation (white arrows in Fig. 8b).

Instead, the slipping zone at the footwall of the secondary hangingwall scarp has a more developed cataclastic fabric (sample AC05_H.F). In fact, few sub-rounded and fractured mm in size clasts and more abundant sub-mm in size angular clasts of the

footwall rocks are dispersed in a dark-brownish in color fine matrix, which becomes more abundant (> 60% in volume) towards the slip surface (Fig. 8c). The latter is continuous and slightly undulated and has a sharp contact with the underlying calcite clasts (Fig 8c, d). Just beneath the slip surface, an about 1 mm thick PSZ made of sub-millimetric in size clasts immersed in a darker fine matrix was identified (Fig. 8d).

Under the scanning electron microscope, the matrix of the PSZ is composed by both large and small packed calcite micro-grains with faint contacts, though straight grain boundaries and triple junctions can still be recognized, and includes clay minerals from the above Holocene matrix (Fig. 8e).

The hangingwall rocks lying on the top of the slip surface are separated from the footwall rocks by a 1-2 mm thick and continuous grey layer made of sub-millimetric in size calcite grains of the underlying PSZ, partially dissolved by karst processes. Indeed, while the contact with the footwall is sharp, the contact of this thin layer with the hangingwall is convoluted. The hangingwall rocks are formed by dm to cm in size almost fracture-free and rounded carbonate clasts cemented by the precipitation of a porous and ochre in color matrix (Fig. 8c, e). This type of microstructure suggests that the hangingwall rocks were cemented *in-situ* and partially preserve the original scarp surface.

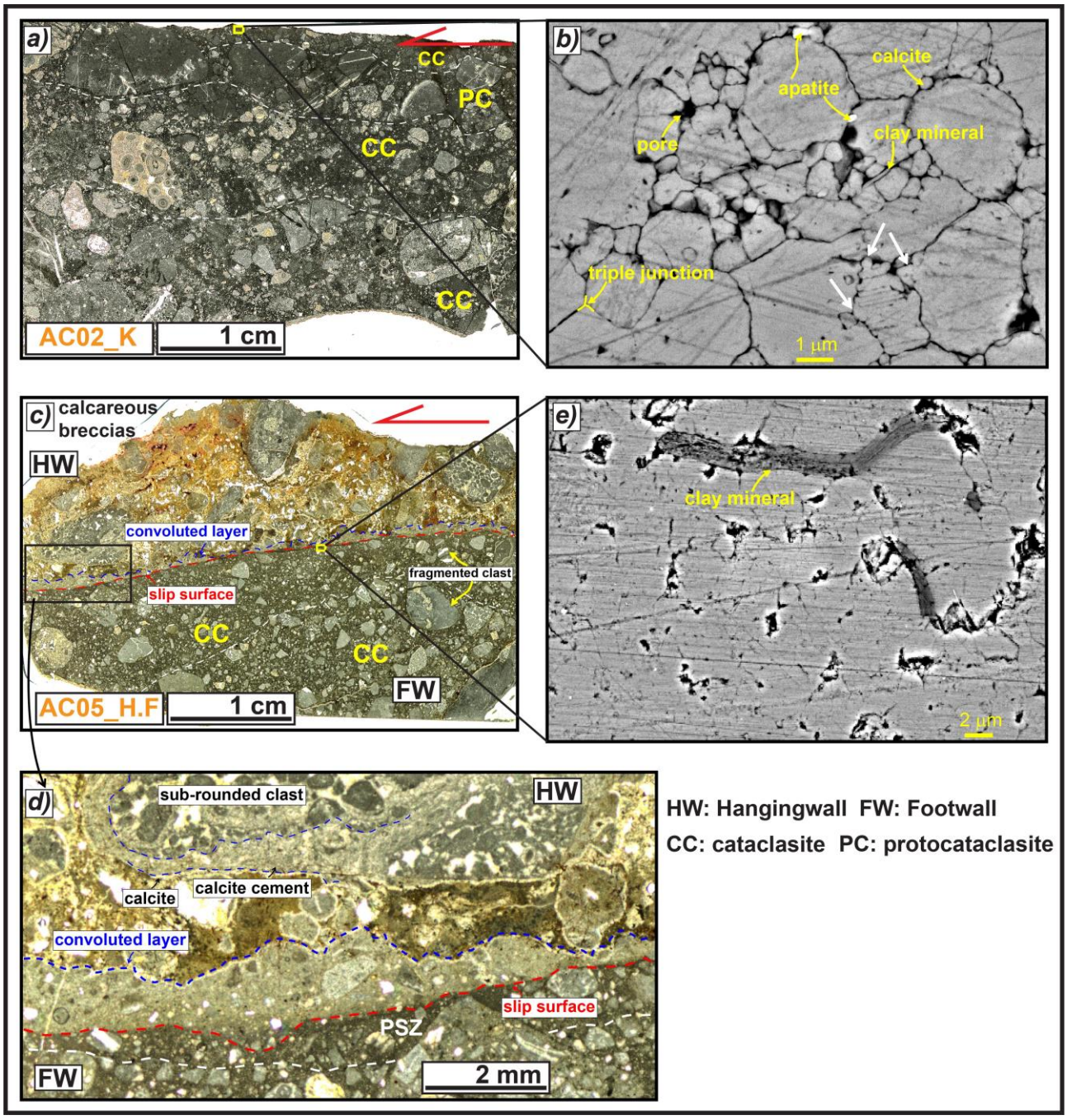

Figure 8: microstructures of the slipping zones relative to the major and secondary scarps of the Alto di Cacchia DGSD. a) Slipping zone of the major scarp, which is made of sub-parallel cataclastic and proto-cataclastic layers, somewhere difficult to identify because of the dark color at optical microscope of the both fine matrix and larger clasts (sample AC02_K). b) SEM image of the fine matrix on the top, formed by packed calcite micro-grains separated by sub-micrometric in size pores and grains of apatite or clay minerals. The grain boundaries are straight, locally forming triple junctions, but somewhere irregular, suggesting grain indentation (white arrows). c) The wall of the secondary scarp includes a well-developed cataclasite at the footwall and fracture-free and cemented calcareous breccias at the hangingwall (sample AC05_H.F). d) The footwall cataclasite includes a < 1 mm thick PSZ and is separated by the hangingwall rocks by a 1-2 mm thick convoluted layer possibly produced by dissolution and precipitation-cementation of the underlying PSZ.

e) SEM image of the matrix from the PSZ, formed by packed calcite micro-grains with faint to straight grain boundaries and including clay minerals of the hangingwall matrix.

Valle Force (relatively small normal fault). The slipping zone in the footwall of the Valle Force normal fault consists of a cataclasite similar to the one described in Fig. 8c of the Alto di Cacchia DGSD, but the slip surface is straighter, with a sharp contact with the underlying clasts (sample VA05_H.F, Fig. 9a-b). The amount of matrix increases towards the slip surface, where the cataclasite is formed by < 1 mm in size sub-rounded clasts and few larger angular clasts oriented with the long axis sub-parallel to the slip surface (Fig. 9a). A < 0.5 mm thick convoluted layer possibly formed by both highly comminuted and almost pore-free packed calcite micro- to nano-grains separates the footwall carbonates from the hangingwall breccias (Fig. 9b-c). The convolute contact with the hangingwall rocks reminds a dissolution-cementation front similar to the one observed in the scarp wall of the Alto di Cacchia DGSD (Fig. 8c, e). In general, the slipping zone at footwall has a cataclastic fabric (from < 1 μm to > 5 μm in grain size) with evidence of clast indentation and rare triple junctions among grains (Fig. 9d). The hangingwall breccias are formed by sub-cm in size sub-rounded to angular carbonate clasts cemented by a brownish porous and fine matrix (Fig. 9a-c, e). The carbonate matrix includes also silica-bearing minerals such as quartz and micas with the long axis oriented sub-parallel to the slip direction (Fig. 9e). This preferential alignment and the size reduction of the grains towards the slip surface is indicative of the involvement of the hangingwall rocks in the fault sliding, but no evidence of mixing structures (e.g., injection or “fluidization” structures; Demurtas et al., 2016) between the hangingwall and footwall rocks was observed (Fig. 9b-d).

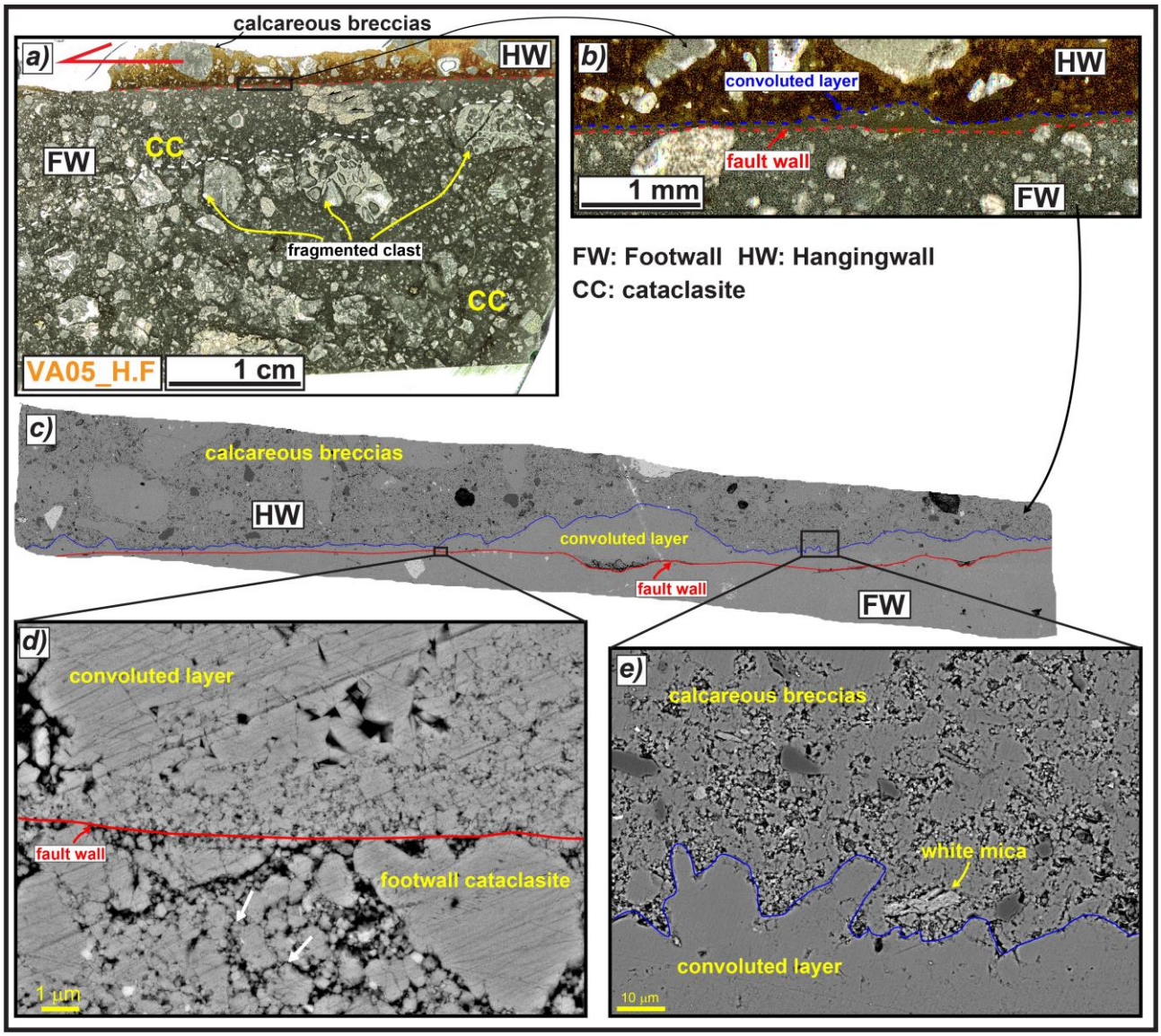

Figure 9: microstructures of the slipping zone along the Valle Force fault wall (sample VA05_H.F). a) Thin section scan of the fault wall, formed by a well-developed cataclasite at the footwall and calcareous breccias at the hangingwall. b-c) Detail of the fault wall, separated by a < 0.5 mm thick convoluted layer lying above the sharp slip surface, possibly formed by dissolution-precipitation processes involving the footwall cataclasite. d) SEM image of the fault wall highlighting the cataclastic fabric of the footwall carbonates, but also the clast indentation (white arrows) and triple junctions among grains. e) SEM Image of the convolute contact between the dissolution-precipitation front and the hangingwall breccias. The latter include angular clasts made of silica-bearing minerals commonly oriented with the long axis sub-parallel to the slip direction.

Sant'Erasmo (DGSD at the footwall of a main seismogenic fault). The slipping zone located in the footwall of the counterslope scarp delimiting to SW the Sant'Erasmo DGSD is a crush breccia to proto-cataclasite formed by cm-to-mm in size rounded clasts immersed in a fine and porous matrix, including fractures sub-parallel and sub-orthogonal to the slip surface (samples SAE02_K and SAE01_K, Fig. 10a, c). The fine reddish matrix

of the hangingwall breccias fills the fractures located just beneath the slip surface and locally is part of a discontinuous cataclastic level (< 5 mm thick) located between the protocataclasite and the slip surface (Fig. 10c). This layer is made of sub-cm and sub-rounded clasts with their long axis oriented sub-parallel to the slip direction, immersed in a brownish ultra-fine matrix (Fig. 10c). The matrix is very porous and is formed by sub-micrometric to micrometric in size grains of calcite and some clay minerals among them (Fig. 10b). The most cemented grains have straight boundaries, locally forming triple junctions, but indentations and sutured contacts are also observed (Fig. 10b; left side of Fig. 10d). The fine matrix is locally cut by calcite veins, with pore spaces locally filled by apatite crystals (right side of Fig. 10d).

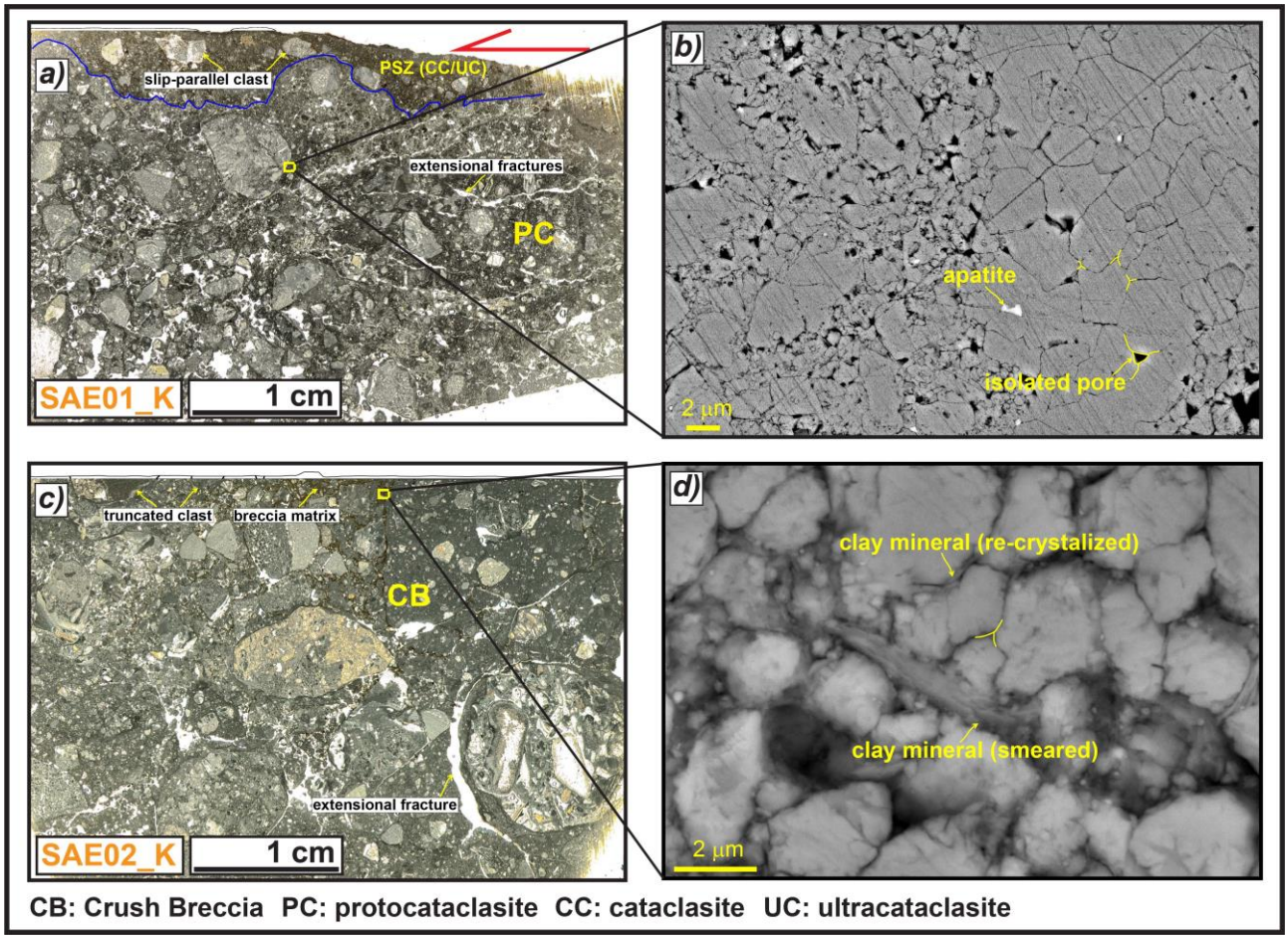

Figure 10: microstructures of the slipping zone of the Sant'Erasmo DGSD counterslope scarp. a) Thin section scan of the slipping zone, a crush breccia formed by cm-to-mm in size rounded clasts (the slip surface was drawn because of the cut of the scan image) (sample SAE01_K). b) SEM image of the hangingwall matrix filling the fractures just beneath the slip surface, formed by packed calcite micro-grains, with straight to irregular boundaries (white arrow) and clay minerals partially filling the pore spaces. c) Thin section scan of the slipping zone where it includes a cataclastic layer close to the slip surface, due to the involvement of the hangingwall matrix into the shearing, formed by < 1 cm in size sub-rounded clasts locally

oriented with their long axis sub-parallel to the slip surface (white arrows) (sample SAE02_K). d) The porous matrix (left side to the dashed line) is formed by locally indented (white arrow) calcite micro-grains with straight contacts, and is cut by veins of calcite, with pore spaces locally filled by apatite crystals (right side).

Mt. Serrone (DGSD at the footwall of a main seismogenic fault). The slipping zone of the Mt. Serrone DGSD is similar to those previously described, as it has a cataclastic fabric formed by cm-to-mm in size angular to sub-rounded clasts immersed in a dark ultra-fine matrix (sample SE01_K, Fig. 11a). The largest clasts are commonly fractured internally and seem as truncated by the slip surface, even though the latter appears quite rough and karstified, thus suggesting possible dissolution and erosion by weathering processes (Fig. 11a). The matrix has a very porous cataclastic appearance with small (<< 1 μm) and large (> 2 μm) in size calcite grains. Similarly to the slipping zones previously described, the calcite grains have straight to stylolitic-like boundaries, locally forming triple junctions and there is widespread evidence of clast indentation (Fig. 11b).

Colle Cerese (DGSD at the footwall of a main seismogenic fault). The slipping zone at the footwall of the Colle Cerese DGSD is a protocataclasite consisting of cm-to-mm in size angular clasts, internally fragmented, immersed in a dark in color ultra-fine and porous matrix (< 40% of the total volume; sample CC01_H.F, Fig. 11c). Though the presence of a cataclastic-like fabric in the matrix and some sort of grain packing is still recognizable (clast indentation, presence of grain boundaries forming triple junctions, etc.) the slipping zone next to the slip surface seems strongly weathered and the pores could be the result also of meteoric exposure and biogenic activities (Fig. 11d). The rough slip surface is preserved by Holocene calcareous breccias, formed by rounded pebbles (> 5 cm in size in the field) poorly cemented by a brownish to white in color calcite-rich matrix, with large cavities filled by sparite (Fig. 11c).

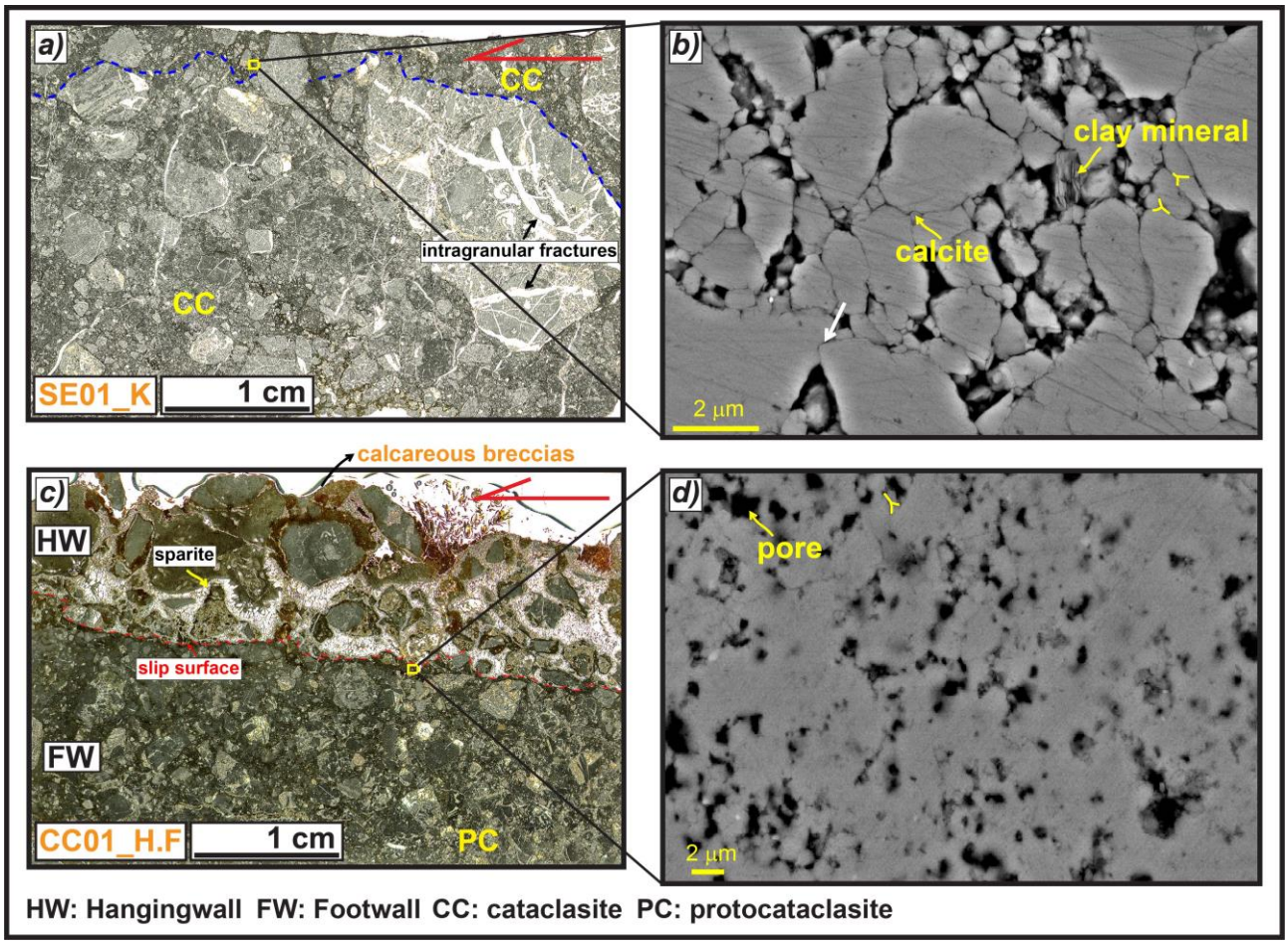

602

603 **Figure 11**: microstructures of the slipping zones of the Mt. Serrone and Colle Cerese DGSDs. a) The
604 slipping zone of the Mt. Serrone DGSD has a cataclastic fabric formed by cm-to-mm in size angular clasts,
605 with the larger ones highly fractured internally, surrounded by a dark-grey fine matrix (sample SE01_K). b)
606 SEM image of the matrix on the top, formed by packed calcite micro-grains, with straight to stylolitic-like
607 boundaries forming triple junctions and indentation structures (white arrow). The empty spaces among the
608 grain boundaries are locally filled by clay minerals. c) Thin section scan of the scarp wall of the Colle Cerese
609 DGSD: a quite rough slip surface delimits a protocataclasite made of calcareous angular to sub-rounded
610 clasts at the footwall with Holocene calcareous breccias cemented by sparite at the hangingwall, which
611 partially preserve the scarp (sample CC01_H.F). d) The fine calcite matrix just beneath the slip surface is
612 very porous, also because of weathering and biogenic activity before sealing from the hangingwall depostis,
613 but clast indentation and triple junctions between grains are still recognizable.

614

615 **San Benedetto-Gioia dei Marsi and Roccapreturo large seismogenic faults.** For
616 comparison with the slipping zones found beneath the sharp surfaces of the DGSDs (Figs.
617 8, 10-11) and the Valle Force fault (Fig. 9), we describe the slipping zones of the major slip
618 surfaces of two large slip seismogenic faults from the same area. The San Benedetto-
619 Gioia dei Marsi (sample Vf01) and Roccapreturo faults (sample Rf01) are both about 10
620 km long segments of the Fucino and the Middle Aterno Valley-Subequana Valley fault
621 systems, capable of producing up to M_w 7.1 and M_w 6.5 earthquakes, respectively (Barchi

et al., 2000; Falcucci et al., 2015) (see also Fig. 14). The core measured in the Venere sector of the San Benedetto-Gioia dei Marsi fault is up to 1 m thick and includes several both matrix- and cemented-supported minor faults (Agosta and Aydin, 2006; Ferraro et al., 2018, 2019). The slipping zone of the major fault surface is a several cm thick cataclasite made of cm-to-mm in size sub-rounded clasts surrounded by a sub-millimetric and dark in color calcite-rich ultra-fine matrix (> 50% in volume).

Both the samples of the slipping zones of the two faults lack of the slip surface. Nevertheless, both the slipping zones include a well-defined, < 0.5 cm thick, cataclastic-ultracataclastic (matrix ca. 80-90% in volume) layer close to the top (Fig. 12a, d). The matrix includes few micrometers to tens of nanometers in size calcite grains with straight to stylolitic-like boundaries and records evidence of grain indentation (Fig. 12b, c). The grain boundaries locally form triple junctions and few isolated pores (Fig. 12b-c, e), rarely filled by apatite crystals in the case of the Roccapreturo fault segment (Fig. 12f).

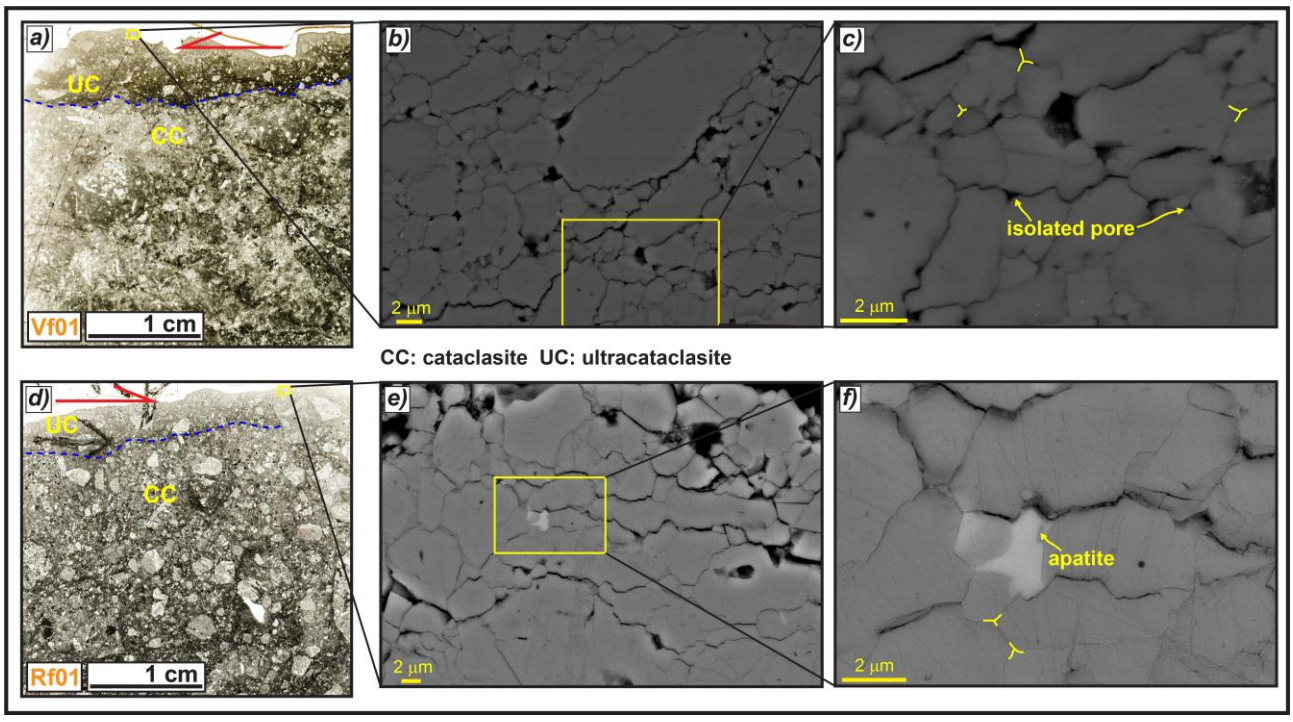

Figure 12: microstructures of the slipping zones relative to the San Benedetto-Gioia dei Marsi (in the Venere sector) and Roccapreturo seismogenic normal fault segments. a) The slipping zone of the San Benedetto-Gioia dei Marsi normal fault has a well-developed cataclastic fabric and includes a well-defined < 0.5 cm thick cataclastic-ultracataclastic layer on the top (sample Vf01). b-c) SEM images of the matrix, formed by highly packed calcite micro- to nano-grains with straight to stylolitic-like contacts, locally forming triple junctions and few isolated pores. d) The slipping zone of the Roccapreturo fault has a similar fabric and also includes an ultracataclastic level on the top (sample Rf01). e-f) SEM images of the matrix from the

644 ultracataclastic level, formed by highly packed calcite micro-grains with straight to irregular contacts
645 separated by small pores, locally filled by apatite crystals.
646

647 5. Discussion

648 In this work we have described 1) the fault/fracture network at footwall of four
649 DGSDs and, for comparison, of a normal fault bordering a relatively small and narrow
650 depression of the central Apennines (section 4.1); 2) the micro- to nano-structures of the
651 slipping zones of the outcropping major and secondary scarps associated to the selected
652 case studies, which were further compared with the slipping zones of two large
653 seismogenic normal faults bordering to SW the DGSDs (section 4.2). Below, we discuss 1)
654 the formation of the DGSDs and the reactivation of the slip surfaces and fracture networks
655 associated (section 5.1) and 2) the deformation mechanisms active in the studied DGSDs
656 hosted in carbonate rocks (section 5.2).
657

658 5.1 Formation and re-activation of the DGSD's fault/fracture networks

659 The fault/fracture networks associated to the DGSDs scarps suggest different loading
660 conditions at the time of their formation. In the case of the Alto di Cacchia, a large number
661 of sub-vertical cracks affect the footwall conglomerates and both the major slip surface
662 and the secondary ones dip on average ~ 70^{o}. Based on the Mohr-Coulomb failure
663 criterion, most of the open fractures should be gravity-induced fractures developed in
664 tensional regime, at very low confining pressures and/or stresses normal to the slip
665 surface (Fig. 13, 14). As a matter of fact, open fractures and other tensional structures like
666 gravitational trenches, ridge top grabens and steep scarps commonly affect the upper and
667 middle portion of DGSDs (Agliardi et al., 2001; Crosta et al., 2013; Cruden & Varnes,
668 1996; Esposito et al., 2007; Gori et al., 2014; Hungr at al., 2014; Mariotto & Tibaldi, 2015).
669 This conclusion is further supported by the observation that this DGSD affects the about
670 400 m thick Pleistocene Cupoli/Aielli Complex, which lies above Cretaceous carbonates.
671 This would suggest that the fault/fracture network formed at very shallow depth ($T < 15\ ^{o}C$
672 and $P_{litho} < 15$ MPa, Fig. 14).
673 In contrast, in the case of the Sant'Erasmo (located at footwall of the Roccapreturo
674 fault), and the Mt. Serrone and Colle Cerese (located at footwall of the San Benedetto-
675 Gioia dei Marsi fault) DGSDs, the joints affecting sub-horizontal Cretaceous limestones
676 have a large scatter in dip and dip angles (Figs. 5-7). This spatial arrangement is
677 consistent with a formation of such fractures at larger confining pressures with respect to

678 the Alto di Cacchia case and possibly under different stress fields (Fig. 13). Nevertheless,
679 the few large sub-vertical open cracks cutting carbonate strata and the absence of veins
680 filling the fractures are features consistent with a recent gravitational activity at shallow
681 surficial conditions. The fault/fracture pattern associated to these DGSDs is similar to the
682 one of the Valle Force fault (Fig. 4) which flattens at 2-3 km of depth on a low angle thrust
683 fault (D'Agostino et al., 1998; Falcucci et al., 2015; Fig. 14). The minor faults and fractures
684 affecting the damage zones of large slip normal faults exhumed from 1-3 km depth (e.g.,
685 San Benedetto-Gioia dei Marsi and Vado di Corno fault zones: Agosta & Kirshner, 2003;
686 Agosta & Aydin, 2006; Demurtas et al., 2016; Figs. 13, 14) have a much higher attitude
687 dispersion, though mainly with strikes oriented NW-SE, consistent with the
688 accommodation of larger strains during the Pleistocene-Holocene extensional phase and
689 dip-slip extensional activity active also at deeper crustal levels (i.e., 2-3 km) .
690 Therefore, according to our interpretation of the structural data here reported,
691 most DGSDs in the central Apennines are the result of gravity induced re-activation of pre-
692 existing minor faults or fractures located at the footwall of larger normal seismogenic
693 faults, well-oriented with respect to the actual stress field. The Alto di Cacchia DGSD in the
694 only one case which has a clear surficial origin, due to the above-mentioned structural
695 features and stratigraphic constraints. In this particular case, the DGSD could be
696 accommodated by both newly formed fractures and faults associated to the slide of
697 Pleistocene cemented conglomerates, or by the re-activation of some fractures associated
698 to faulting, possibly even seismic, at very shallow depths (200-300 m at maximum) (Fig.
699 14).
700 The major scarps delimiting the Alto di Cacchia, Mt. Serrone and Sant'Erasmo
701 DGSDs (< 500 m long) are ~ 3 m high (Figs. 3, 5 and 6), whereas the ones of the Valle
702 Force fault and Colle Cerese DGSD (> 1 km in length) locally reach 8 m and 10 m of
703 height, respectively (Figs. 5, 7). Such large height scarp values are comparable to the
704 ones of most scarp outcropping in central Apennines and associated to large normal faults
705 (up to 10 km in length along-strike and accommodating up to 600 m of maximum throw;
706 Ferraro et al., 2018). Moreover, the scarps of these DGSDs appear very sharp and,
707 locally, smooth, although strongly karstified, as well as most of the scarps of active
708 seismogenic normal faults in the central Apennines (Agosta & Aydin 2006; Galadini and
709 Galli, 2000; Smeraglia et al., 2017). This would imply that high and sharp outcropping
710 scarps can be produced either by gravitational processes or by tectonic, possibly seismic,
711 faulting, or by a combination of them.

In conclusion, the major sharp scarps delimiting the studied DGSDs are pre-existing fault/fracture surfaces developed in the footwall of large seismogenic faults, re-activated by gravitational displacement. The higher angle fractures initially allowed the formation of ridge top grabens and gravitative trenches at the slope crest (Chigira, 1992; Crosta et al., 2013; Gori et al., 2014; Mariotto & Tibaldi, 2015; Savage & Varnes, 1987). Then, the initial rock-mass spreading evolves into a large sliding, with the basal surface of the Sackung DGSD that flattens at depth (few hundreds of meters) or link with other possible lower angle fractures closer to the master fault (e.g., P-shear fractures or preexisting thrust faults.). The rotational sliding causes the development of rock topples, trenches and uphill-facing scarps on the middle sector of the slope (Agliardi et al., 2001; Chigira, 1992; Cruden & Varnes, 1996; Varnes, 1978;). At the DGSD toe (unfortunately, not exposed in the studied area), the increase of the compressional forces due to the increment of the normal stress acting on the sub-horizontal slip surface causes the bulging of the rock-mass (Chigira, 1992; Hermann et al., 2000; Mariani & Zerboni., 2020; Savage & Varnes, 1987; Zischinsky, 1968). In the Colle Cerese and Sant'Erasmo DGSDs, where the carbonate strata dip in the opposite direction of the slope (i.e., anaclinal slope), the Sackung-type DGSD produce scarps, uphill-facing scarps, and show a large double ridge morphology (Moro et al., 2009; Figs. 2, 14). In the Mt. Serrone DGSD, instead, where the bedding dips in the same direction of the slope (i.e., cataclinal slope) the double ridge is less-developed and series of steep downhill- and uphill-facing scarps delimiting small grabens and gravitative trenches affect the entire slope (Cruden, 1989; Hermann et al., 2000; Mariani & Zerboni, 2020; Moro et al., 2012; Figs. 2, 14). The Alto di Cacchia DGSD, instead, is accommodated by steeper scarps cutting sub-horizontal conglomerates, which probably re-use pre-existing faults developed in the underlying carbonates.

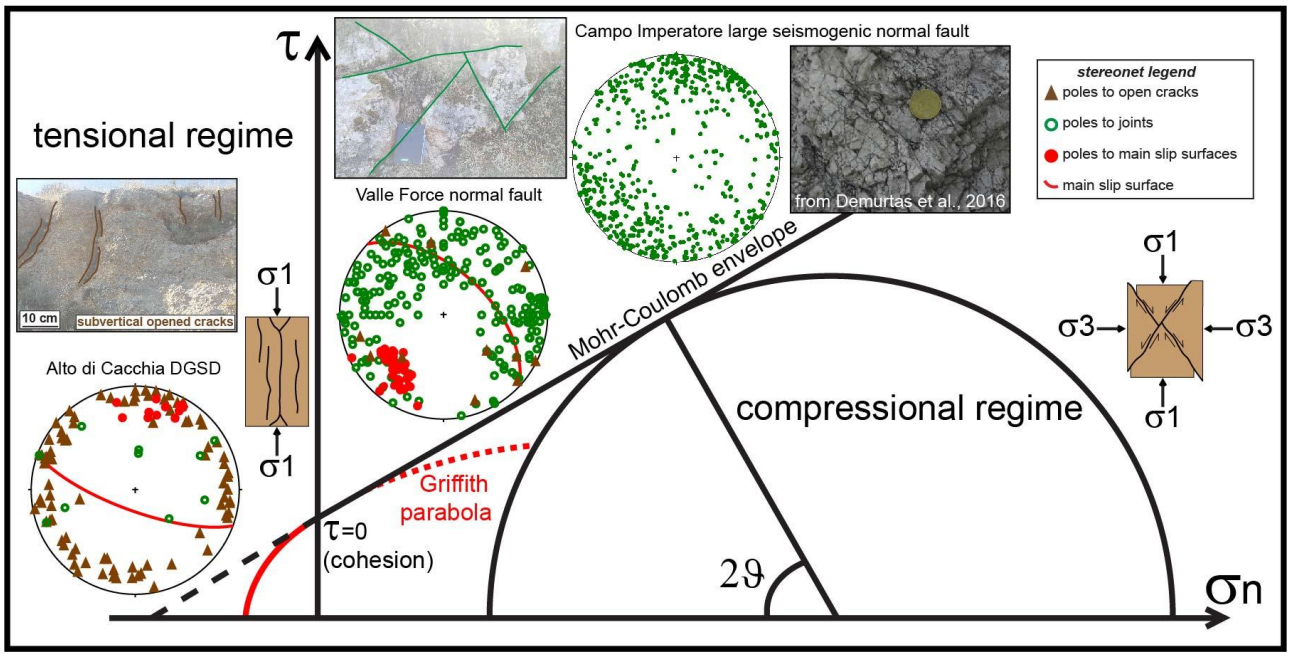

Figure 13: stereonets showing the poles of the joints and open fractures at footwall of the Alto di Cacchia DGSD, Valle Force normal fault and the Vado di Corno seismogenic fault (Campo Imperatore fault system, Demurtas et al., 2016; Fondriest et al., 2020) and their relation with the orientation of newly formed fractures according to the Morh-Coulomb failure criteria in the Mohr space. The open cracks dipping at > 70° ("high angle") crosscutting the footwall rocks of the Alto di Cacchia DGSD were reasonably formed under a tensional regime, at very low confining pressures. The conjugated joints affecting the Valle Force fault scarp and the footwall rocks have a dip angle which is consistent with their formation at higher confining pressures with respect to the Alto di Cacchia DGSD. The high scatter of the attitude of joints affecting the Vado di Corno fault core, most of them striking NW-SE, is consistent with the accommodation of larger strains during the last extensional phase and deeper normal dip slip activity of the structure, exhumed from > 1 km of depth.

5.2 Deformation mechanisms in carbonate-hosted DGSDs

The slipping zones at footwall of the DGSDs and of the Valle Force fault scarps have quite similar microstructures, in particular when observed at micrometric scale (Figs. 8-11). At this scale, the textures of the fine matrix are also similar to the ones found in the slipping zones of the San Benedetto-Gioia dei Marsi and Roccapreturo seismogenic normal fault segments (Fig. 12), suggesting the activation of similar deformation mechanisms. Here, we will relate the microstructures of the DGSDs slipping zones and the ones of the normal faults with the main deformation mechanisms active on carbonate rocks at crustal conditions.

Evidence from the slipping zones microstructures. In active seismogenic normal faults, the bulk of displacement during co-seismic slip is mainly accommodated by slipping

zones including millimetric thick zones of extreme localization (Chester et al., 1993; Chester & Chester, 1998; Power & Tullis, 1989; Sibson, 2003). The major slip surfaces of the large slip San Benedetto-Gioia dei Marsi and Roccapreturo seismogenic fault segments have a several cm-thick cataclastic slipping zone in which the strain is extremely localized in a ~ 0.5 cm thick ultracataclastic layer (Fig. 12a, d). In addition, the cm-thick slipping zones of the Vado di Corno fault surface (Campo Imperatore seismogenic fault system) contain mixed clasts and gouges deriving from both the hangingwall Quaternary deposits and the footwall Mesozoic carbonates arranged in “fluidization structures” or injections from the slipping zone into the wall rocks (see Fig. 3c and 11c of Demurtas et al., 2016).

In contrast, the slipping zones at footwall of the scarps of the Mt. Serrone, Colle Cerese and Sant’Erasmo DGSDs have a protocataclastic fabric and lack of a well-defined cataclastic-ultracataclastic level towards the slip surface (Figs. 10a, 11a, c). Moreover, the slipping zones of the Valle Force fault (Fig. 9a) and Alto di Cacchia DGSD (Fig. 8c) are similar to each other; indeed, they consist of a well-developed footwall cataclasite delimited from the hangingwall breccias by a sharp slip surface. Nevertheless, the slip surface of the Alto di Cacchia DGSD, as well as the one of the Colle Cerese DGSD, appears rougher than the one of Valle force fault. Furthermore, in both the slipping zones of the Colle Cerese and Alto di Cacchia DGSDs there is no evidence of “fluidization” or injections structures and of intense mixing between the hangingwall and footwall blocks. In addition, the hangingwall breccias appears as almost totally undeformed and highly cemented (Fig. 8c, 11c). This would suggest a possible emplacement, and subsequent *in-situ* cementation, of the Quaternary hangingwall rocks just after the exhumation of the scarp (Fig. 8c, 11c). Instead, the Pleistocene breccias at the hangingwall of the Valle Force fault were involved in the sliding, as suggested by the grain size reduction toward the fault surface and the preferential orientation parallel to the slip surface of the silicate minerals of the matrix. However, the strain rates in the slipping zones were probably too low to induce an intense mixing between the two fault blocks (Fig. 9b, c).

In conclusion, at the slipping zone scale, the major active seismogenic faults differ from DSGDs because of their well-developed cataclastic fabric, which include extreme localization in ultracataclastic layers, thick cataclasites sealed by a dense calcite-vein network and mixing of footwall and hangingwall materials. Some of these features can be also found in the slipping zone of the smaller (few kilometers long both along-dip and along-strike) Valle Force fault. It seems that these features can be associated to the larger

slip accommodated by these faults with respect to the DGSDs. But other than this, there are no clear evidence regarding the microstructural organization of the slipping zones which allowed us to distinguish DGSDs from tectonic faults. Moreover, since we interpret the DGSDs scarps as pre-existing minor faults located at footwall of larger normal faults, the microstructures observed in the DGSDs slipping zones could be mainly produced by tectonic, instead of gravitational sliding. Further studies need to be carried out in order to get more constraints on the exhumation depth of these fault rocks, as for example detailed clumped isotopes analyses on matrix and cements.

Evidence from the matrix of the slip zones. Cataclastic and ultracataclastic layers and their associated slip surfaces are the location of the most extreme deformation in faults. As a consequence, the associated microstructures, and in particular those relative to the fine matrix, may yield information on the deformation mechanisms active during faulting and DGSD.

At the micro-scale, the matrix of the slip zones at footwall of the Valle Force fault and of the four DGSDs major scarps is formed by calcite micro- to nano-grains, with straight to stylolitic grain boundaries forming locally triple junctions and isolated pores with widespread clast indentation (Figs. 8b, e; 9d; 10b, d; 11b). The matrix of the ultra-cataclastic layers of the San Benedetto-Gioia dei Marsi and Roccapreturo seismogenic fault segments shows a texture quite similar to the one described above, even though the grain boundaries among calcite grains are straighter, the triple junctions more widespread and the pore spaces smaller (compare Figs. 8b, 9d, 10b, d and 11b, d with Fig. 12b, e). Although similar, this fabric differs from the typical foam-like fabric produced in laboratory by shearing at seismic velocities (i.e. > 0.1 m/s) carbonate-built fault gauges (Demurtas et al., 2019; Fondriest et al., 2013; Pozzi et al., 2019; Smith et al., 2013; Verberne et al., 2013). Indeed, the latter experimentally-produced fabric consists on highly packed micro-grains of calcite with straight contacts forming triple junctions at 120° and very small or absent pore spaces. In these experimental studies, given also the high temperatures measured in the slip zones during shearing, the main deformation mechanism proposed is Grain Boundary Sliding (GBS) aided by diffusion creep (De Paola et al., 2015; Pozzi et al., 2019), which activates at T > 550°.

Natural and experimental observations have shown that chemical compaction by pressure-solution driven by fluid-rock interactions can be the main process of porosity loss in carbonates, in particular in calcite-rich rocks (Croizè et al., 2013; Ferraro et al., 2019;

Gratier er al., 2013, 2015; Meyers and Hill, 1983; Renard et al., 2000; Rutter, 1983; Scholle and Halley, 1985; Tada & Seiver, 1989). Pressure-solution occurs in presence of a liquid phase through dissolution at grain contacts, diffusion of the solute matter and precipitation of the latter within the pore spaces. The process is mainly driven by the stress acting at the grain-to-grain contact and does not require high ambient pressures and temperatures to be activated (Croize et al., 2013; Gratier et al., 2013, 2015; Rutter, 1983; Tada and Siever, 1989).

According to these observations, the cataclastic-like fabric observed in the matrix of the slipping zones associated to both normal faults and DGSDs suggest pressure-solution processes occurring at very low temperatures and confining pressures (i.e., $T < 15^{o}$, $P_{litho} <$ 15 MPa). Cataclastic flow processes cause clast comminution by frictional sliding, grain crushing and micro-cracks growth. The subsequent ingression and percolation of fluids within the pore spaces (e.g., Lucca et al., 2019) among the calcite grains cause a very efficient pressure-solution process resulting in grain indentation and stylolitic-like grain boundaries, pore space reduction and precipitation within the fractures closest to the dissolution areas of newly calcite grains and secondary phases (Agosta et al., 2012; Bathurst, 1971; Carrio-Schaffhauser et al., 1990; Croize et al., 2013; Renard & Ortoleva, 1997; Rutter, 1983). The grain size is one of the main factors in controlling the rate of pressure-solution, because the smaller the grains, the shorter is the path of the solute matter to the precipitation site (Ferraro et al., 2019; Lehner, 1990; Renard et al., 2000; Rutter, 1983; Tada and Siever, 1989). Indeed, the slipping zones of the San Benedetto-Gioia dei Marsi and Roccapreturo normal fault segments underwent more pressure-solution than the ones of the Valle Force fault and of the DGSDs probably because of the smaller average size of the grains.

The slip zones of the DGSDs and associated karstified sharp to smooth slip surfaces are often affected by weathering (incipient formation of rillenkarren, micro-holes due to organic activity, etc.) as further attested by the formation of continuous but irregular boundaries between well-cemented layers close to the principal slip surfaces that can be interpreted as dissolution-precipitation fronts (Fig. 8e, 9b).

The major slip surface of the Valle Force fault shows ultra-polished patches where the hangingwall breccias are removed and has a sharp contact with the underlying clasts (fig. 4e). the ultra-polished surface patches could be the result of crack propagation within already lithified fault rocks and abrasion associated to the formation of Y-shears in calcite-rich gouge that smooth the slip surface, followed by the activation of pressure-solution

dissolving the finer grain size leaving behind a polished surface (e.g., Mercuri et al., 2018; Tesei et al., 2017). alternatively, ultra-polished slip surfaces might be the result of extreme coseismic localization at larger crustal depths (Demurtas et al., 2016; De paola et al.,2015; Fondriest et al., 2013; Pozzi et al., 2018) overprinted by low-temperature pressure-solution compaction during interseismic periods and exhumation. this would suggest that, in fluid-saturated systems, ultra-polished slip surfaces are likely produced by fluid-driven and low temperature diffusive processes active on smooth slip surfaces formed during either seismic or aseismic slip. Recent experiments by Rempe et al. (2020) indicate that seismic slip is not able to induce crystal plasticity on carbonate gouges and to produce localized slip surfaces at low effective stresses (i.e., < 2 MPa) in the presence of pressurized pore fluids. instead, carbonate fluid-saturated gouges sheared at very low effective stresses likely deform by granular and, to a less extent, cataclastic flow during earthquakes. these experimental results may thus be relevant to interpret the origin of localized slip surfaces within fluid-saturated deposits which were not affected by significant burial (< 400 m); this might be the case of the Alto di Cacchia.

In conclusion, in spite of the different depth of formation and loading conditions, both carbonate-hosted normal faults and DGSDs have similar microstructures. The latter are here interpreted, based on high resolution microstructural investigations, as the result of cataclastic flow fragmentation associated to seismic or aseismic slip concomitant or followed by low temperature fluid-driven diffusive processes.

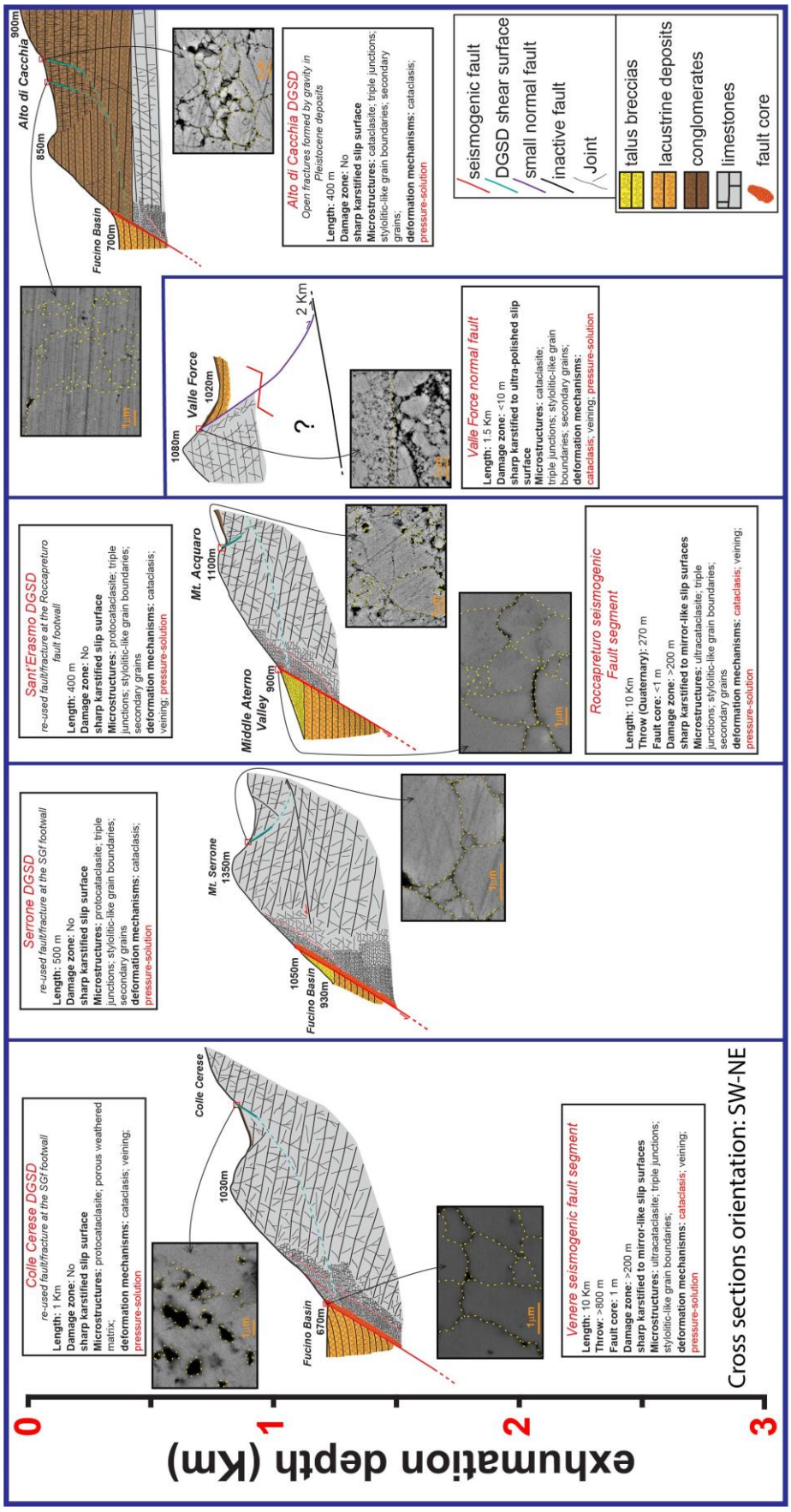

Figure 14: Geological cross sections and main characteristics of the studied cases (displacement of the slip surface, common microstructures associated, inferred deformation mechanisms, exhumation depth of the

fault/fracture network, etc.). The San Benedetto-Gioia dei Marsi and Roccapreturo fault zones exhumed from > 1 km of depth. The Valle Force normal fault exhumed from shallower depths and flattens at about 2 km of depth on a pre-existing thrust. The major slip surfaces of the DGSDs re-activate pre-existing faults and fractures at the footwall of the associated large normal faults. The microstructures of the slip zones are very similar in both normal faults and DGSDs, suggesting low temperature diffusive processes (i.e., pressure-solution) as the dominant deformation mechanism active at shallow depth in carbonates.

7. Conclusions

In the Italian central Apennines, sharp, often karstified, slip surfaces displace carbonate rocks and accommodate either seismic ruptures or Deep-seated-Gravitational-Slope-Deformations (DGSDs). We analyzed the cases of the Alto di Cacchia, Sant'Erasmo, Colle Cerese and Mt. Serrone DGSDs, located at the footwall of large slip seismogenic normal faults and the case of the Valle Force, a < 2 km long normal fault bordering a karst depression (Figs. 1, 2). At the footwall of the major scarp delimiting the Alto di Cacchia DGSD, numerous open cracks, largely scattered in attitude, were measured, consistent with a surficial formation of this structure (i.e., < 500 m) (Figs. 3, 13). Instead, the fault/fracture network associated to the other selected DGSDs consist of both open and closed fractures, often arranged in conjugated sets, and scattered in dip and dip angles, indicative of a deeper formation depth (i.e., > 1 km of depth) and recent gravitational activity (Figs. 4-7, 13). In fact, such fracture distribution is similar to the one of the Valle Force fault (Figs. 4, 13), which flattens at 2-3 km depth along a low angle inactive thrust fault (Fig. 14). Therefore, we interpret most DGSDs slip surfaces in the central Apennines as a gravitational re-use of pre-existing minor faults and fractures at footwall of the associated larger normal faults exhumed from 1-3 km depth (Figs. 13, 14). Gravitative trenches, ridge top grabens and tensional cracks affect the upper portion of the slope. Due to the flattening of the basal sliding surface, the lateral spreading evolves into a Sackung-type DGSD with associated topples, scarps and up-hill facing scarps in the middle portion of the slope, with associated more or less developed double ridges (Figs. 2, 14).

The maximum height values (from 3 to 10 meters) of the scarps delimiting the DGSDs are comparable to the ones of the main (up to 10 km of length along-strike) seismogenic central Apennines normal faults. Therefore, well-exposed high and sharp slip surfaces, also in large seismogenic faults, can be related to both faulting or karst/gravity-induced processes. Other parameters, such as the along-strike length and continuity of the outcropping scarp, the associated geomorphological features (e.g., double crest ridge, up-hill facing scarps or gravitational trenches), the earthquakes distribution, the focal

mechanisms in the area and the relationships of the outcropping slip surfaces with the other neighboring structures are the best parameters to interpret the association of the scarps with gravitational or tectonic processes.

At centimetric scale, the slipping zones of the large slip San Benedetto-Gioia dei Marsi and Roccapreturo seismogenic normal faults have a cataclastic fabric and include a ~ 0.5 cm thick continuous ultracataclastic layer just beneath the slip surface (Figs. 12a, d). In contrast, the slipping zones at footwall of the Sant'Erasmo, Colle Cerese and Mt. Serrone DGSDs have a protocataclastic fabric and commonly lack of a well-defined cataclastic-ultracataclastic layer under the slip surface (Sant'Erasmo and Colle Cerese: Figs. 10a, 11c) or, where present, they are thin and discontinuous (Sant'Erasmo and Mt. Serrone: Figs 10c, 11a). The slipping zones at footwall of the Alto di Cacchia DGSD and of the Valle Force fault surfaces, instead, have a well-developed cataclastic fabric, but lack of a well-defined ultracataclastic layer on the top. The well-developed and thicker slipping zones associated to the large normal faults can be explained by the larger amount of slip accommodated by the latter compared to the DGSDs.

At micrometric scale, in both normal faults and DGSDs the fine matrix has a cataclastic-like aspect formed by highly packed and indented calcite micro to nano-grains with both straight and indented or even stylolitic-like grain boundaries (Figs. 8-11). This fabric is the result of cataclasis occurring by clast fragmentation and frictional sliding and low temperature pressure-solution processes (i.e., $T < 15^{o}$, $P < 15$ MPa). The main difference in the calcite-rich matrix of the investigated slipping zones is the intensity of packing (e.g., abundance of triple junctions, indentation, pores and pore size). The calcite micro-grains forming the matrix of the large slip normal faults are more packed because of the smaller average grain size, which favors the process of pressure-solution.

Our work stresses the general microstructural convergence of micro-scale processes active on seismic faults and DGSDs, with the activation of both cataclastic flow and pressure-solution producing smooth to polished slip surfaces. Therefore, detailed characterization of the footwall fracture network distribution and evolution, together with geomorphological features, are key parameters to interpret the association of slip scarps with gravitational or tectonic driven processes.

Acknowledgments

This research was funded by the European Research Council Consolidator Grant Project NOFEAR No 614705 (L.D.R., M.F. and G.D.T.); by two INGV projects: "Caratterizzazione microstrutturale di piani di faglia attivi ed esumati e di piani di scivolamento di deformazioni

gravitative profonde di versante (DGPV)" and "Investigation of bedrock shear planes microstructures" and by a Marie Curie Fellowship (M.M). Thank Leonardo Tauro for thin section preparation, Nicola Michelon for preparing field materials and Telemaco Tesei for comments on the microstructures.

Author contributions

M.M., M.S., S.G., E.F., G.D.T., L.D.R. and M.F. conceived the original idea; F.D. drone imaging; L.D.R., M.F., M.M., S.G., E.F. and G.D.T. field work; L.D.R. and A.C. microstructural analyses; L.D.R., G.D.T. and M.F. microstructural interpretation; L.D.R. wrote the manuscript with input from G.D.T., M.M., S.G., E.F. and M.F. All authors discussed the results and commented on the manuscript.

None of the data in our manuscript has been published or is under consideration elsewhere. The collected dataset was uploaded and is available on http://researchdata.cab.unipd.it/

References

Agliardi, F., Crosta, G., & Zanchi, A. (2001). Structural constraints on deep-seated slope deformation kinematics. *Engineering Geology*, 59, 83-102.

Agliardi, F., Crosta, G. B., & Frattini, P. (2012). Slow rock-slope deformation. In: Clague, J.J., Stead, D. (Eds.), *Landslides Types, Mechanisms and Modeling* (pp. 207-221). Cambridge: Cambridge University Press.

Agliardi, F., Scuderi, M., Fusi, N., & Collettini, C. (2020). Slow-to-fast transition of giant creeping rockslides modulated by undrained loading in basal shear zones. *Nature Communications*, 11, 1352. https://doi.org/10.1038/s41467-020-15093-3

Agosta, F., & Kirschner, D. (2003). Fluid conduits in carbonate-hosted seismogenic normal faults of central Italy. *J. Geophys. Res.,* 108(B4), 2221. http://dx.doi.org/10.1029/2002JB002013.

Agosta, F., & Aydin, A. (2006). Architecture and deformation mechanism of a basin bounding normal fault in Mesozoic platform carbonates, central Italy. *J. Struct. Geol.*, 28(8), 1445-1467.

Agosta, F., Ruano, P., Rustichelli, A., Tondi, E., Galindo-Zaldivar, J., & De Galdeano, C. S. (2012). Inner structure and deformation mechanisms of normal faults in conglomerates and carbonate grainstones (Granada Basin, Betic Cordillera, Spain): inferences on fault permeability. *J. Struct. Geol.,* 45, 4-20.

Ambrosi, C., & Crosta, G.B. (2006). Large sackung along major tectonic features in the Central Italian Alps. *Engineering Geology*, 83, 183-200.

Ambrosi, C., & Crosta, G.B. (2011). Valley shape influence on deformation mechanisms of rock slopes. In: Jaboyedoff, M. (Ed.), Slope Tectonics. *Geological Society, London, Special Publications* 351(1), 215-233.

Arignoli, D., Gentili, B., Materazzi, M., & Pambianchi, G. (2010). Deep-seated gravitational slope deformations in active tectonics areas of the Umbria-Marche Apennine (central Italy). *Geogr. Fis. Dinam. Quat*., 33, 127-140.

Barchi, M., Galadini, F., Lavecchia, G., Messina, P., Michetti, A. M., Peruzza, L., Pizzi, A., Tondi, E., & Vittori, E. (2000). Sintesi delle conoscenze sulle faglie attive in Italia Centrale: parametrizzazione ai fini della caratterizzazione della pericolosità sismica. CNR Gruppo Nazionale per la Difesa dai Terremoti, Roma, 62.

Bathurst, R. G. C. (1971). *Carbonate Sediments and Their Diagenesis*. Amsterdam-Oxford-New York: Elsevier.

Bianchi Fasani, G., Di Luzio, E., Esposito, C., Evans, S. G., & Scarascia Mugnozza, G. (2014). Quaternary, catastrophic rock avalanches in the Central Apennines (Italy): Relationships with inherited tectonic features, gravity-driven deformations and the geodynamic frame. *Geomorphology*, 211, 22-42.

Billi, A., & Storti, F. (2004). Fractal distribution of particle size in carbonate cataclastic rocks from the core of a regional strike-slip fault zone. *Tectonophysics,* 384(1), 115-128.

Boncio, P., Lavecchia, G., & Pace, B. (2004). Defining a model of 3D seismogenic sources for seismic hazard assessment applications: the case of central Apennines (Italy). *Journal of Seismology*, 8(3), 407-425.

Bosi C., & Messina P. (1991). Ipotesi di correlazione fra successioni morfo-litostratigrafiche plio-pleistoceniche nell'Appennino Laziale-Abruzzese. *Studi Geol. Cam.*, Special Vol. 1991/2, 257-263.

Bosi, C., Galadini, F., Giaccio, B., Messina, P., & Sposato, A. (2003). Plio-Quaternary continental deposits in the Latium-Abruzzi Apennines: the correlation of geological events across different intermontane basins. *Il Quaternario,* 16, 55-76.

Caine, J. S., & Forster, C. B. (1999). Fault Zone Architecture and Fluid Flow: Insights from Field Data and Numerical Modeling. *American Geophysical Union Geophysical Monograph*, 113, 101-127.

Calamita, F., Coltorti, M., Farabollini, P., & Pizzi, A. (1994). Le faglie normali Quaternarie nella Dorsale Appenninica Umbro-Marchigiana: proposta di un modello di tettonica di inversione. *Studi Geol. Camerti*, 1, 211-225.

Calamita, F., Pizzi, A., Scisciani, V., De Girolamo, C., Coltorti, M., Pieruccini, P., & Turco, E. (2000). Caratterizzazione delle faglie quaternarie nella dorsale appenninica umbro-marchigiano-abruzzese. In: F. Galadini, C. Meletti, and A. Rebez (Eds.), *Le Ricerche del GNDT Nel Campo Della Pericolosità Sismica (1996–1999) (pp. 157-169)*, CNR-Gruppo Nazionale per la Difesa dai Terremoti, Roma.

Carafa, M. M. C., Galvani, A., Di Naccio, D., Kastelic, V., Di Lorenzo, C., Miccolis, S., et al. (2020). Partitioning the ongoing extension of the central Apennines (Italy): Fault slip rates and bulk deformation rates from geodetic and stress data. *Journal of Geophysical Research: Solid Earth*, 125. https://doi.org/ 10.1029/2019JB018956

Carminati E., & Doglioni C. (2012). Alps vs. Apennines: the paradigm of a tectonically asymmetric Earth. *Earth Sci. Rev.*, 112(1–2), 67-96.

Carminati, E., Lustrino, M., & Doglioni, C. (2012). Geodynamic evolution of the central and western Mediterranean: Tectonics vs. igneous petrology constraints. *Tectonophysics,* 579, 173-192.

Carrio-Schaffhauser, E., Raynaud, S., Latiere, H. J., & Mazerolles, F. (1990). Propagation and localization of stylolites in limestones. In: Knipe, R.J., Rutter, E. H. (Eds.), Deformation Mechanisms, Rheology and Tectonics. *Geological Society, London, Special Publications*, 54, 193-199.

Castellarin, A., Colacicchi, R., & Praturlon, A. (1978). Fasi distensive, trascorrenze e sovrascorrimenti lungo la “linea Ancona-Anzio”, dal Lias medio al Pliocene. *Geologica Romana,* 17, 161-189.

Cavinato, G. P., Carusi, C., Dall’Asta, M., Miccadei, E., & Piacentini, T. (2002). Sedimentary and tectonic evolution of Plio-Pleistocene alluvial and lacustrine deposits of the Fucino Basin (central Italy). *Sedimentary Geology,* 148, 29-59.

Chester, F. M., Biegel, R. L., & Evans, J. P. (1993). Internal structure and weakening mechanisms of the San-Andreas fault. *J. Geophys. Res: Solid Earth,* 98, 771-786.

Chester, F. M., & Chester, J. S. (1998). Ultracataclasite structure and friction processes of the Punchbowl fault, San Andreas system, California. *Tectonophysics*, 295, 199-221.

Chiaraluce, L. (2012). Unravelling the complexity of Apenninic extensional fault systems: A review of the 2009 L’Aquila earthquake (central Apennines, Italy), *J. Struct. Geol.,* 42, 2-18.

Chiaraluce, L., Di Stefano, R., Tinti, E., Scognamiglio, L., Michele, M., & Casarotti, E. (2017). The 2016 Central Italy seismic sequence: A first look at the mainshocks, aftershocks, and source models. *Seismological Research Letters*, 88(3), 757-771. https://doi.org/10.1785/0220160221

Chigira, M. (1992). Long-term gravitational deformation of rock by mass rock creep. *Engng Geol*, 32(3), 157-184.

Chigira, M., Wu, X., Inokuchi, T., Wang, G. (2010). Landslides induced by the 2008 Wenchuan earthquake, Sichuan, China. *Geomorphology,* 118, 225-238.

Cipollari, P., Cosentino, D., Esu, D., Girotti, O., Gliozzi, E., & Praturlon, A. (1999a). Thrust-top lacustrine-lagoonal basin development in accretionary wedges: late Messinian (Lago-Mare) episode in the central Apennines (Italy). *Palaeogeogr. Palaeoclimatol. Palaeoecol.,* 151, 146-166.

Cosentino, D., Cipollari, P., Marsili P., & D. Scrocca (2010). Geology of the central Apennines: a regional review, In: M. Beltrando, A. Peccerillo, M. Mattei, S. Conticelli and C. Doglioni (Eds.), *The Geology of Italy*, *J. Virt. Explor*., 36, paper 11.

Croize, D., Renard, F., & Gratier, J. P. (2013). Compaction and porosity reduction in carbonates: a review of observations, theory, and experiments. *Adv. Geophys.*, 54, 181-238.

Crosta, G. B., Frattini, P., & Agliardi F. (2013). Deep seated gravitational slope deformations in the European Alps. *Tectonophysics*, 605, 13-33.

Cruden D. M., & Varnes D. J. (1996). Landslide types and processes. In: Turner AK, Schuster RL (Eds.) *Landslides investigation and mitigation* (pp. 36-75). Washington DC: US Geological survey fact sheet

Damiani, A. V., Chiocchini, M., Colacicchi, R., Mariotti, G., Parotto, M., Passeri, L., & Praturlon, A. (1992). Elementi litostratigrafici per una sintesi delle facies carbonatiche meso-cenozoiche dell'Appennino centrale. *Studi Geologici Camerti*, Vol. spec. 1991/2, 187-213.
Demangeot, J. (1965). Ge`omorphologie des Abruzzes Adriatiques. Centre Recherche et Documentation Cartographiques Memoires et Documents, Numero hors serie, 403.

Della Seta, M., Esposito, C., Marmoni, G. M., Martino, S., Scarascia Mugnozza, G., & Troiani, F. (2017). Morpho-structural evolution of the valley-slope systems and related implications on slope-scale gravitational processes: New results from the Mt. Genzana case history (Central Apennines, Italy). *Geomorphology, 289, 60-77.*

Dramis, F., & Sorriso-Valvo, M. (1994). Deep-seated gravitational slope deformations, related landslides and tectonics. *Engineering Geology*, 38, 231-243.

D'Agostino, N., Chamot-Rooke, N., Funiciello, R., Jolivet, L., & Speranza, F. (1998). The role of pre-existing thrust faults and topography on the styles of extension in the Gran Sasso range (central Italy), *Tectonophysics*, 292, 229-254.

D'Agostino, N., Giuliani, R., Mattone, M., & Bonci, L. (2001). Active crustal extension in the central Apennines (Italy) inferred from GPS measurements in the interval 1994-1999. *Geophysical Research Letters,* 28, 2121-2124.

D'Agostino N., Mantenuto S., D'Anastasio E., Giuliani R., Mattone M., Calcaterra S., Gambino P., & Bonci L. (2011). Evidence for localized active extension in the central Apennines (Italy) from global positioning system observations. *Geology,* 39, 291-294, 10.1130/G31796.1

Demurtas, M., Fondriest, M., Balsamo, F., Clemenzi, L., Storti, F., Bistacchi, A., & Di Toro, G. (2016). Structure of a normal seismogenic fault zone in carbonates: the Vado di Corno fault, Campo Imperatore, central Apennines (Italy). *J. Struct. Geol.,* 90, 185-206. https://doi.org/10.1016/j.jsg.2016.08.004

Demurtas M., Smith S., Prior D., Brenker F., & Di Toro G. (2019). Grain size sensitive creep during simulated seismic slip in nanogranular fault gouges: constraints from Transmission Kikuchi Diffraction (TKD). *J. of Geoph. Res.* 127, 10197-10209, 10.1029/2019JB018071.

De Paola, N., Holdsworth, R. E., Viti, C., Collettini, C., & Bullock, R. (2015). Can grain size sensitive flow lubricate faults during the initial stages of earthquake propagation? *Earth Planet. Sci. Lett.*, 431, 48-58. https://doi.org/10.1016/j.epsl.2015.09.002.

Doglioni, C. (1995). Geological remarks on the relationships between extension and convergent geodynamic settings. *Tectonophysics,* 252, 253-267.

Elter, P., Giglia, G., Tongiorgi, M., & Trevisan, L. (1975). Tensional and compressional areas in the recent (Tortonian to present) evolution of the Northern Apennines. *Bollettino di Geofisica Teorica ed Applicata*, 17, 3-18.

EMERGEO Working Group (2010). Evidence for surface rupture associated with the Mw 6.3 L'Aquila earthquake sequence of April 2009 (central Italy). *Terra Nova*, 22, 43-51.

Esposito, C., Martino, S., & Scarascia Mugnozza, G. (2007). Mountain slope deformations along thrust fronts in jointed limestone: An equivalent continuum modelling approach. *Geomorphology*, 90, 55-72.

Evans, S. G., & Clague, J. J. (1994). Recent climatic change and catastrophic geomorphic processes in mountain environments. *Geomorphology*, 10, 107-128.

Falcucci E., Gori S., Moro M., Pisani A. R., Melini D., Galadini F., & Fredi P. (2011). The 2009 L'Aquila earthquake (Italy): what next in the region? Hints from stress diffusion analysis and normal fault activity. *Earth and Planetary Science Letters*, 305, 350-358.

Falcucci, E., Gori, S., Moro, M., Fubelli, G., Saroli, M., Chiarabba, C., & Galadini, F. (2015). Deep reaching versus vertically restricted Quaternary normal faults: Implications on seismic potential assessment in tectonically active regions. Lessons from the middle Aterno valley fault system, central Italy. *Tectonophysics*, 305, 350-358. https://doi.org/10.1016/j.tecto.2015.03.021

Falcucci, E., Gori, S., Galadini, F., Fubelli, G., Moro, M., & Saroli, M. (2016). Active faults in the epicentral and mesoseismal Ml 6.0 24, 2016 Amatrice earthquake region, central Italy. Methodological and seismotectonic issues. *Annals of Geophysics,* 59, track 5, doi:10.4401/ ag-7266

Ferraro F., Agosta, F., Ukar, E., Grieco D. S., Cavalcante F., Belviso C., & Prosser, G. (2019). Structural diagenesis of carbonate fault rocks exhumed from shallow crustal depths: An example from the central-southern Apennines, Italy. *Journal of Structural Geology*, 122, 58-80.

Fondriest, M., Smith S. A., Candela T., Nielsen S. B., Mair K., & Di Toro G. (2013). Mirror-like faults and power dissipation during earthquakes, *Geology*, 41(11), 1175-1178.

Fondriest, M., Aretusini, S., Di Toro, G., & Smith, S. A. F. (2015). Fracturing and rock pulverization along an exhumed seismogenic fault zone in dolostones: The Foiana Fault Zone (Southern Alps, Italy). *Tectonophysics,* 654, 56-74.

Galadini, F. (1999). Pleistocene changes in the central Apennine fault kinematics: A key to decipher active tectonics in central Italy. *Tectonics*, 18(5), 877-894.

Galadini, F., & Galli, P. (2000). Active tectonics in the central Apennines (Italy) — input data for seismic hazard assessment. *Natural Hazards,* 22, 225-270.

Galadini F., Meletti, G., & Vittori, E. (2000). Stato delle conoscenze sulle faglie attive in Italia: elementi geologici di superficie. In: F. Galadini, C. Meletti, and A. Rebez (Eds.), *Le Ricerche del GNDT Nel Campo Della Pericolosità Sismica (1996–1999) (pp. 107-136)*, CNR-Gruppo Nazionale per la Difesa dai Terremoti, Roma.

Galadini, F., Messina, P., Giaccio, B., & Sposato, A. (2003). Early uplift history of the Abruzzi Apennines (central Italy): available geomorphological constraints. *Quaternary International*, 101-102, 125-135.

Galadini, F., & Messina, P. (2004). Early-middle Pleistocene eastward migration of the Abruzzi Apennine (central Italy) extensional domain. *Journal of Geodynamics*, 37, 57-81.

Galadini, F. (2006). Quaternary tectonics and large-scale gravitational deformations with evidence of rock-slide displacements in the Central Apennines (central Italy). *Geomorphology*, 82, 201-228.

Giraudi, C. (2001). I sedimenti di riempimento di piccole conche sulle morene dell'Appennino Centrale: un contributo alla comprensione delle variazioni ambientali postglaciali. *Italian Journal of Quaternary Sciences*, 14(2), 131-136.

Gori, S., Falcucci, E., Dramis, F., Galadini, F., Galli, P., Giaccio, B. et al. (2014). Deep-seated gravitational slope deformation, large-scale rock failure, and active normal faulting along Mt. Morrone (Sulmona basin, Central Italy): Geomorphological and paleoseismological analyses. *Geomorphology,* 208, 88-101.

Gratier, J. P., Dysthe, D., & Renard, F. (2013). The role of pressure solution creep in the ductility of the Earth's upper crust. *Adv. Geophys.,* 54, 47-179.

Gratier, J. P., Noiriel, C., & Renard, F. (2015). Experimental evidence for rock layering development by pressure solution. *Geology*, 43, 871-874.

Hermann, S. W., Madritsch, G., Rauth, H., & Becker, L. P. (2000). Modes and Structural Conditions of Large-Scale Mass Movements (Sackungen) on Crystalline Basement Units of the Eastern Alps (Niedere Tauern, Austria). *Mitt, naturwiss. Ver. Steiermark,* 130, 31-42.

Hungr O., Leroueil, S., & Picarelli, L. (2014). The Varnes classification of landslide types, an update. *Landslides,* 11, 167-194.

Jahn, A. (1964). Slow morphological features resulting from gravitation. *Zeitschr. Geomorph.,* 5, 59-72.

Jibson, R.W., Harp, E. L., Schulz, W., & Keefer, D. K. (2004). Landslides triggered by the 2002 Denali fault, Alaska earthquake and the inferred nature of the strong shaking. *Earthquake Spectra,* 20, 669-691.

Lehner, F. K. (1990). Thermodynamics of rock deformation by pressure solution. In: Barber, D. J., Meredith, P. G. (Eds.), *Deformation Processes in Minerals, Ceramics and Rocks*. London, United Kingdom: Unwin Hyman Ltd.

Malinverno, A., & Ryan, W. B. F. (1986). Extension in the Tyrrhenian Sea and shortening in the Apennines as result of arc migration driven by sinking of the lithosphere. *Tectonics,* 5, 227-245.

Mancinelli, P., Porreca, M., Pauselli, C., Minelli, G., Barchi, M. R., & Speranza, F. (2019). Gravity and magnetic modeling of Central Italy: Insights into the depth extent of the seismogenic layer. *Geochemistry, Geophysics, Geosystems,* 20, 2157-2172. https://doi.org/10.1029/2018GC008002

Mariani G. S., & Zerboni, A. (2020). Surface Geomorphological Features of Deep-Seated Gravitational Slope Deformations: A Look to the Role of Lithostructure (N Apennines, Italy). *Geosciences*, 10, 334. doi:10.3390/geosciences10090334

Mariotto F. P., & Tibaldi A. (2015). Inversion kinematics at deep-seated gravity slope deformations: a paleoseismological perspective. *Nat. Hazards Earth Syst. Sci. Discuss.*, 3, 4585-4617. doi:10.5194/nhessd-3-4585-2015

Mariucci M. T., & Muller B. (2003). The tectonic regime in Italy inferred from borehole breakout data. *Tectonophysics,* 361, 21-35.

Martel, S. J. (2006). Effect of topographic curvature on near-surface stresses and application to sheeting joints. *Geophysical Research Letters*, 33. doi:10.1029/2005GL024710, 2006

McCalpin, J. P. (1999). *Criteria for determining the seismic significance of sackungen and other scarp-like landforms inmountainous regions. Techniques for Identifying Faults and Determining their Origins*. Washington, DC: U.S. Nuclear Regulatory Commission.

Meyers, W. J., & Hill, B. E. (1983). Quantitative studies of compaction in Mississippian skeletal limestones, New Mexico. *J. Sediment. Petrol.,* 53, 231-242.

Mercuri, M., Scuderi, M., Tesei, T., Carminati, E., & Collettini, C. (2018). Strength evolution of simulated carbonate bearing faults: The role of normal stress and slip velocity. *J. Struct. Geol.,* 109, 1-9.

Molnar, P. (2004). Interactions among topographically induced elastic stress, static fatigue, and valley incision. *Journal of Geophysical Research*, 109. http://dx.doi.org/10.1029/2003JF000097.

Morewood N. G., & Roberts G. P. (2000). The geometry, kinematics and rates of deformation within an en échelon normal fault segment boundary, central Italy. *Journal of Structural Geology,* 22, 1027-1047.

Moro, M., Saroli, M., Salvi, S., Stramondo, S., & Doumaz, F. (2007). The relationship between seismic deformation and deep-seated gravitational movements during the 1997 Umbria–Marche (Central Italy) earthquakes. *Geomorphology*, 89, 297-307.

Moro, M., Saroli, M., Tolomei C., & Salvi, S. (2009). Insights on the kinematics of deep-seated gravitational slope deformations along the 1915 Avezzano earthquake fault (Central Italy), from time-series DInSAR *Geomorphology,* 112, 261-276.

Moro, M., Saroli, M., Gori, S., Falcucci, E., Galadini, F., & Messina, P. (2012). The interaction between active normal faulting and large scale gravitational mass movements revealed by paleoseismological techniques: A case study from central Italy. *Geomorphology,* 151-152, 164-174.

Panek, T., & Klimeš, J. (2016). Temporal behavior of deep-seated gravitational slope deformations: A review. *Earth-Science Reviews*, 156, 14-38.

Pánek, T., Táborík, P., Klimeš, J., Komárková, V., Hradecký, J., & Šťastný, M., 2011a. Deep-seated gravitational slope deformations in the highest parts of the Czech Flysch Carpathians: evolutionary model based on kinematic analysis, electrical imaging and trenching. *Geomorphology*, 129, 92-112.

Parotto, M. & Praturlon, A. (1975). Geological summary of the central Apennines. *Quaderni de 'La Ricerca Scientifica' 90*, 257-311.

Pizzi, A., C., Coltorti, M., & Pieruccini, P. (2002). Quaternary normal faults, intramontane basins and seismicity in the Umbria-Marche-Abruzzi Apennine ridge (Italy): Contribution of neotectonic analysis to seismic hazard assessment. *Boll. Soc. Geol. It*., 1, 923-929.

Pollard, D. & Aydin, A. (1988). Progress in understanding jointing over the past century: *Geological Society of America Bulletin*, 100, 1181-1204.

Pozzi, G., De Paola, N., Holdsworth, R. E., Bowen, L., Nielsen, S. B., & Dempsey, E. D. (2019). Coseismic ultramylonites: an investigation of nanoscale viscous flow and fault weakening during seismic slip. *Earth Planet. Sci. Lett*., 516, 164-175.

Power, W. L., & Tullis, T. E. (1989). The relationship between slickenside surfaces in fine grained quartz and the seismic cycle. *J. Struct. Geol*., 11(7), 879-893. doi:10.1016/0191-8141(89) 90105-3.

Renard, F., & Ortoleva, P. J. (1997). Water films at grain-grain contacts: Debye-Huckel osmotic model of stress, salinity, and mineralogy dependence. *Geochem. Cosmochim*., Acta 61, 1963-1970.

Renard, F., & Gratier, J. P., Jamtveit B. (2000). Kinetics of crack-sealing, intergranular pressure solution, and compaction around active faults *J. of Struct. Geol.,* 22(10), 1395-1407.

Rempe, M., Di Toro, G., Mitchell T. M., Smith S. A. F., Hirose T., & Renner J. (2020). Influence of effective stress and pore-fluid pressure on fault strength and slip localization in carbonate slip zones. *Journal of Geophysical Research: Solid Earth*, 10.1029/2020JB019805, JGRB54497 in press.

Roberts, G. P., & Michetti, A. M. (2004). Spatial and temporal variations in growth rates along active normal fault systems: an example from the Lazio–Abruzzo Apennines, central Italy. *Journal of Structural Geology,* 26, 339-376.

Royden, L., & Patacca, E., & Scandone, P. (1987). Segmentation and configuration of subducted lithosphere in Italy: an important control on thrust-belt and foredeep basin evolution. *Geology,* 15, 714-717.

Rovida, A., Locati, M., Camassi, R., Lolli, B., & Gasperini, P. (2020). The Italian earthquake catalogue CPTI15. *Bulletin of Earthquake Engineering*, 18, 2953-2984. https://doi.org/10.1007/s10518-020-00818-y

Rutter, E. H. (1983). Pressure solution in nature, theory and experiment. *J. Geol. Soc. Lond.,* 140, 725-740.

Sammis C. G., King G., & Biegel R. (1987). The kinematics of gouge deformation. *Pure Appl. Geophys.,* Vol. 125, 777-812.

Savage, W. Z., & Varnes, D. J. (1987). Mechanics of gravitational spreading of steep-sides ridges (sackung). *IAEG Bull.*, 35, 31-36.

Scholle, P. A., & Halley, R. B. (1985). Burial diagenesis: out of sight, out of mind. In: *Carbonate Cements*, 36, Society of Economic Paleontologists and Mineralogists, 309-334.

Serpelloni E., Anzidei M., Baldi P., Casula G., & Galvani A. (2005). Crustal velocity and strain-rate fields in Italy and surrounding regions: new results from the analysis of permanent and non-permanent GPS networks. *Geophys J. Int*., 161(3), 861-880.

Sibson, R. H. (2003). Thickness of the seismic slip zone, Bull. *Seismol. Soc. Am.,* 93, 1169-1178.

Siman-Tov, S., Aharonov, E., Sagy, A., & Emmanuel S. (2013). Nanograins form carbonate fault mirrors. *Geology*, 41, 703-706.

Smeraglia, L., Billi, A., Carminati, E., Cavallo, A., & Doglioni C. (2017a). Field-to nano-scale evidence for weakening mechanisms along the fault of the 2016 Amatrice and Norcia earthquakes, Italy. *Tectonophysics,* 712-713, 156-169.

Smeraglia, L., Bettucci, A., Billi, A., Carminati, E., Cavallo, A., Di Toro, G., Natali, M., Passeri, D., Rossi, M., & Spagnuolo, E. (2017b). Field-to nano-scale evidence for weakening mechanisms along the fault of the 2016 Amatrice and Norcia earthquakes, Italy. *Tectonophysics,* 712-713, 156-169.

Smith, S. A. F., Di Toro, G., Kim, S., Ree, J. H., Nielsen, S., Billi, A., & Spiess, R. (2013). Coseismic recrystallization during shallow earthquake slip. *Geology, 41*, 63-66.

Stampfli G., & Finetti I. R., Plate tectonics of the Apulia-Adria microcontinents, Atlases in Geosciences. CROP PROJECT: Deep Seismic Exploration of the Central Mediterranean and Italy, 2005 Amsterdam Elsevier 747-766.

Stramondo, S., Saroli, M., Moro, M., Atzori, S., Tolomei, C., & Salvi, S. (2005). Monitoring long term ground movements and Deep Seated Gravitational Slope Deformations by InSAR time series: cases studies in Italy. Extended Abstract in Proceedings ESA Esrin, 28 November - 2 December 2005, Frascati, Italy http://earth.esa.int/fringe2005/

Tada, R., & Siever, R. (1989). Pressure solution during diagenesis. Annu. Rev. *Earth Planet Sci.*, 17, 89-118.

Tesei, T., Carpenter, B. M., Giorgetti, C., Scuderi, M., Sagy, A., Scarlato, P., & Collettini, C. (2017). Friction and scale-dependent deformation processes of large experimental carbonate faults. *J. Struct. Geol*., 100, 12-23. http://dx.doi.org/10.1016/j.jsg.2017. 05.008.

Tozer, R. S. J., Butler R. W. H., & Corrado S. (2002). Comparing Thin- and Thick-Skinned thrust tectonic models of the central Apennines, Italy, *Stephan Mueller Spec. Publ. Ser.*, 1, 181-194.

Valensise, G., & Pantosti D. (2001). Database of potential sources for earthquakes larger than M 5.5 in Italy. *Annali di Geofisica*, 44, 287-306.

Varnes, D. J. (1978). Slope movements types and processes. In: Schuster, R.L., Krizek, R.J. (Eds.), *Landslides: Analysis and Control* (11-35).

Verberne, B. A., Spiers, C. J., Niemeijer, A. R., De Bresser, J. H. P., De Winter, D. A. M., & Plümper, O. (2013). Frictional properties and microstructure of Calcite-rich fault gouges sheared at sub-seismic sliding velocities. *Pure Appl. Geophys*., 171 2617-2640. http://dx.doi.org/10.1007/s00024-013-0760-0.

Vezzani, L., & Ghisetti, F. (1998). Carta Geologica dell'Abruzzo, scala 1:100.000. Regione Abruzzo, settore urbanistica-beni ambientali e cultura. S.EL.CA., Firenze.

Vezzani, L., Festa, A., & Ghisetti, F. C. (2010). Geology and tectonic evolution of the Central-Southern Apennines, Italy. *Geological Society of America, Special Paper,* 469, 1-58.

Ward, S. N. & Valensise, G. (1989). Fault Parameters and slip distribution of the 1915 Avezzano, Italy, earthquake derived from geodetic observations, *Bull. Seismol. Soc. Am.,* 79, 690-710.

Zischinsky, U. (1966). On the deformation of high slopes. *Ist Conf. Int. Soc. Rock Mech*., 2, 179-185.

Zischinsky, U. (1969). *Uber Sackungen*. *Rock Mechanics*, 1, 30-52.